



Drell-Yan production in Parton Branching method at low and high DY masses

Qun Wang

in collaboration with

A. Bermudez Martinez, P. Connor, D. Dominguez Damiani, L. Estevez Banos, F. Hautmann, H. Jung, J. Lidrych, A. Lelek, M. Schmitz, S. Taheri Monfared, H. Yang

DESY & Peking University

30/07/2020

ICHEP 2020 | PRAGUE

40th INTERNATIONAL CONFERENCE
ON HIGH ENERGY PHYSICS

**VIRTUAL
CONFERENCE**

28 JULY - 6 AUGUST 2020

PRAGUE, CZECH REPUBLIC

Outline

- ❖ TMDs and Parton Branching (PB) method
- ❖ Application in Drell-Yan (DY) production
 - ❖ DY production at LHC
 - ❖ DY production at low mass

[1]. F. Hautmann, H. Jung, A. Lelek, V. Radescu, and R. Zlebcik. “Soft-gluon resolution scale in QCD evolution equations”. *Phys. Lett.*, B772:446451, 2017.

[2]. F. Hautmann, H. Jung, A. Lelek, V. Radescu, and R. Zlebcik. “Collinear and TMD Quark and Gluon Densities from Parton Branching Solution of QCD Evolution Equations”. *JHEP*, 01:070, 2018.

[3]. A. Bermudez Martinez, P. Connor, F. Hautmann, H. Jung, A. Lelek, V. Radescu, and R. Zlebcik. “Collinear and TMD parton densities determined from fits to HERA DIS measurements”, DESY-18-042

[4] A. Bermudez Martinez, P. Connor, D. Dominguez Damiani, L. Estevez Banos, F. Hautmann, H. Jung, J. Lidrych, M. Schmitz, S. Taheri Monfared, Q. Wang, R. Zlebcik. “Production of Z-bosons in the Parton branching method”, *PRD*. 100.074027, arXiv:1906.00919

[5] A. Bermudez Martinez, P. Connor, D. Dominguez Damiani, L. Estevez Banos, F. Hautmann, H. Jung, J. Lidrych, A. Lelek, M. Schmitz, S. Taheri Monfared,, Q. Wang, T. Wening, H. Yang, R. Zlebcik. “The transverse momentum spectrum of low mass Drell-Yan production at next-to-leading order in the Parton Branching method”, arXiv:2001.06488

TMD

- ❖ TMDs (Transverse Momentum Dependent parton distributions)
 - ❖ Transverse momentum effects are naturally coming from intrinsic k_t and parton showers
 - ❖ **New approach: Parton Branching method**
 - ❖ Determine integrated PDF from parton branching solution of evolution equation
 - ❖ Cover all transverse momenta from small k_t to large k_t as well a large range in x and μ^2
 - ❖ provide a novel method to solve evolution equations.
 - ❖ Determine TMD:
 - ❖ Since each branching is generated explicitly, energy-momentum conservation is fulfilled and transverse momentum distributions can be obtained

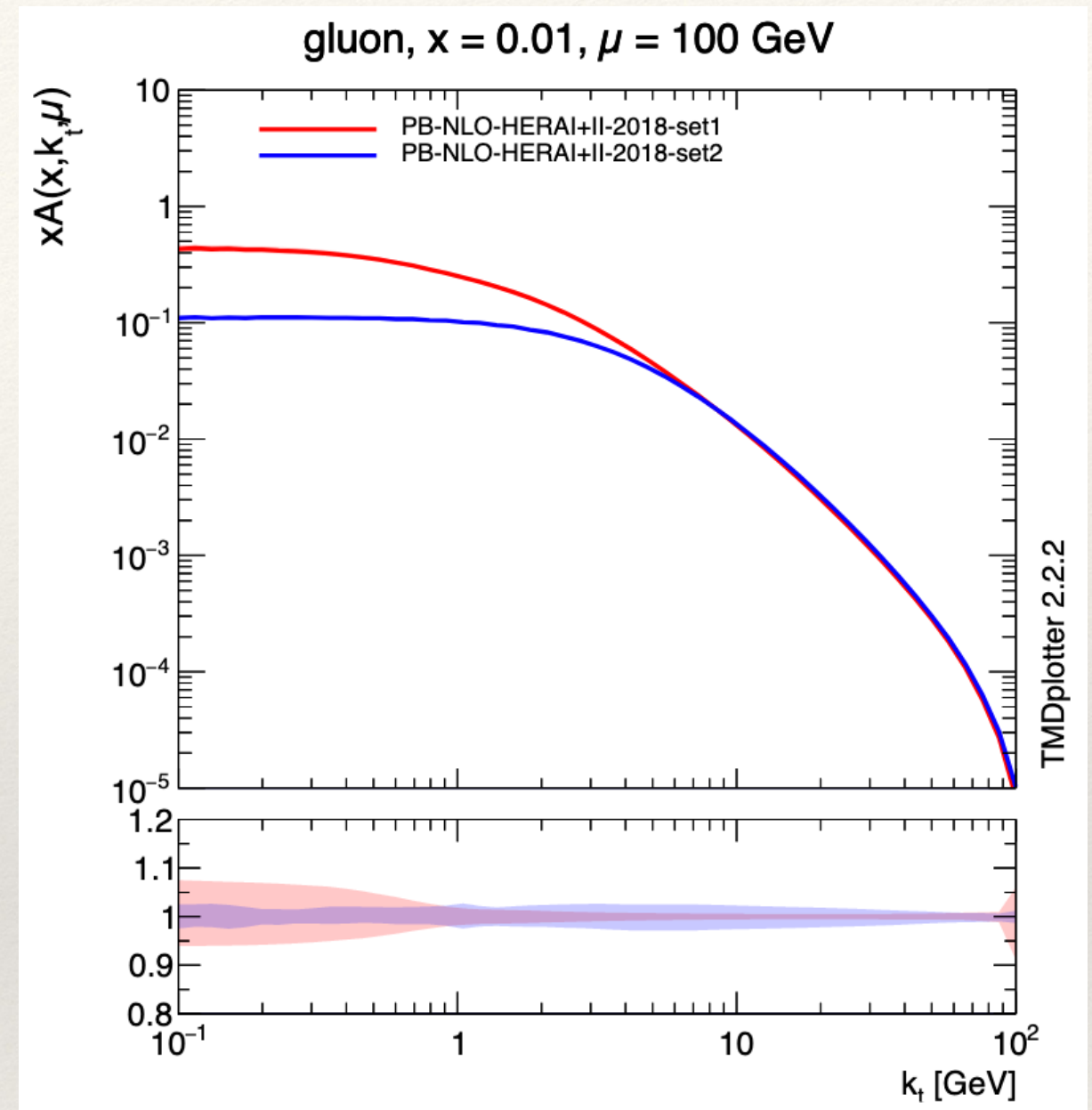
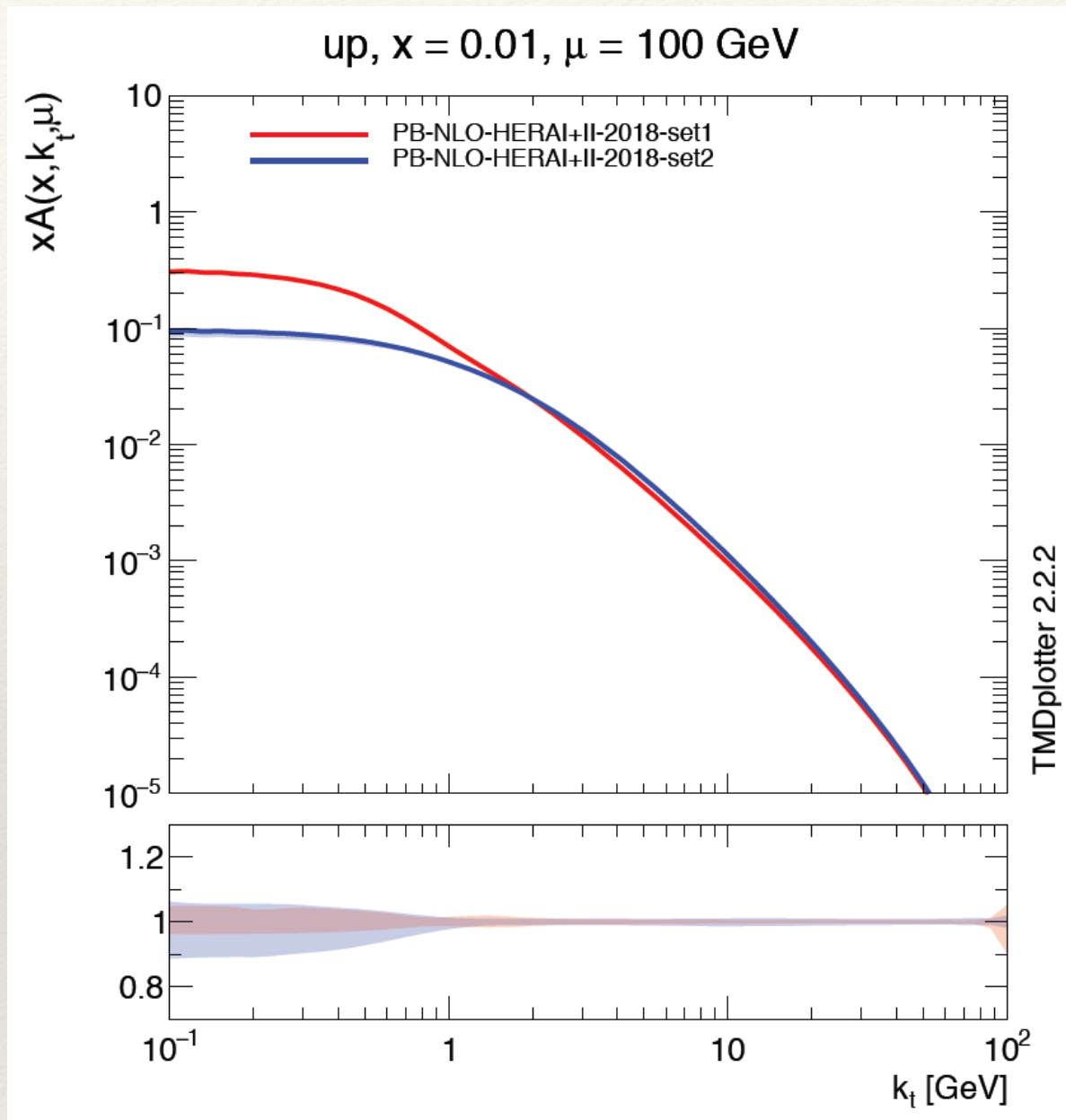
TMD

- ❖ Parton Branching evolution generates every single branching:
 - ❖ Kinematics can be calculated at every step

- ❖ Fit performed using xFitter frame (with collinear Coefficient functions at NLO)
 - ❖ using full HERA 1+2 inclusive DIS (neutral current, charged current) data
 - ❖ in total 1145 data points **——more details in Sara's talk**
 - ❖ Kinematic range:
 $3.5 < Q^2 < 50000 \text{ GeV}^2, 4 \times 10^{-5} < x < 0.65$
 - ❖ Using starting distribution as in HERAPDF2.0
 $\chi^2/ndf = 1.2$

—> Can be easily extended to include any other measurement for fit!

TMD distributions



- ❖ Difference essentially in low k_T region
 - ❖ experimental and model uncertainties obtained from fit, small
 - ❖ at very low k_T , uncertainties from intrinsic k_T sizable

Application to Drell-Yan production

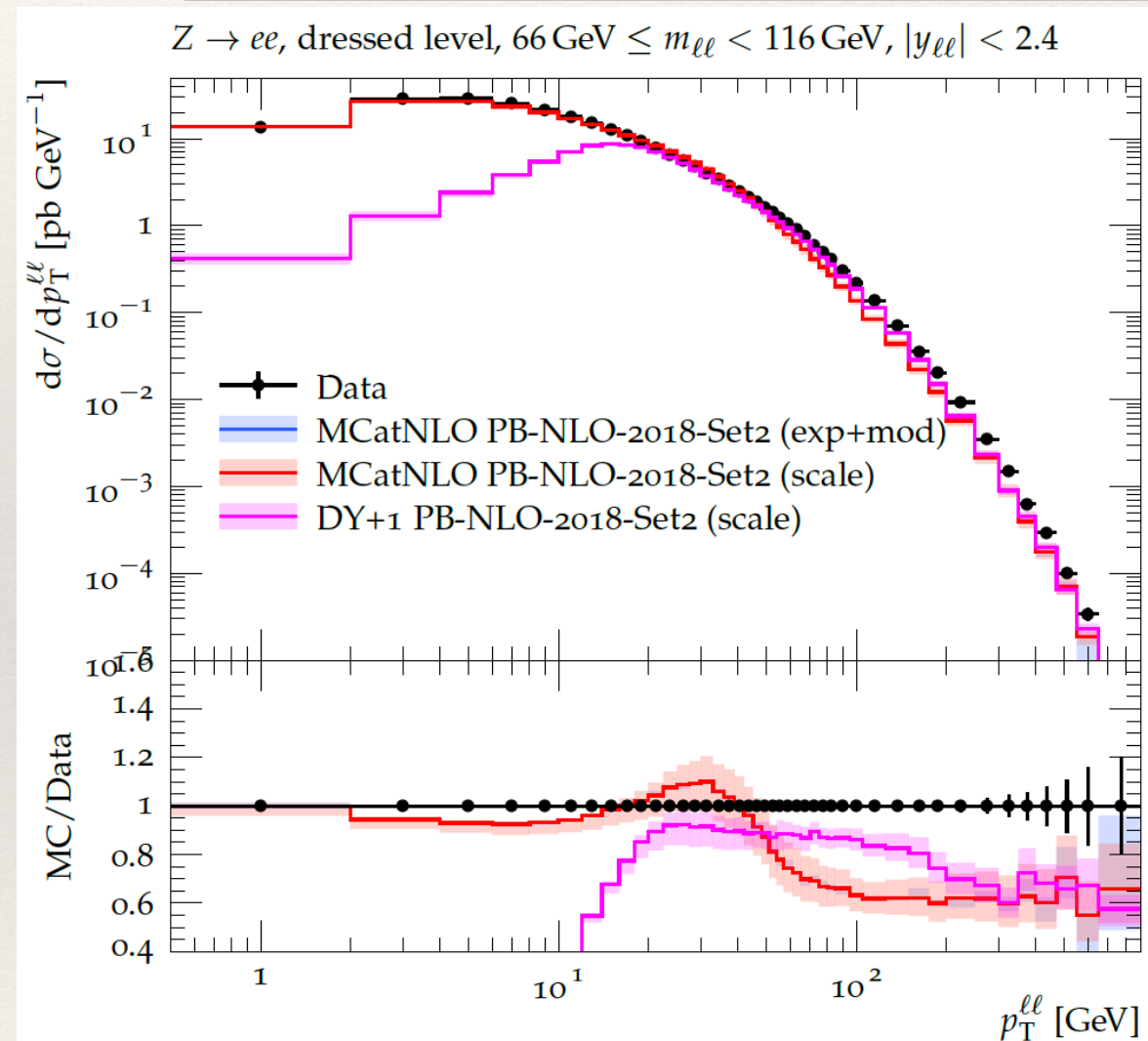
- ❖ Application in Drell-Yan (DY) production
 - ❖ DY production at LHC
 - ❖ DY production at low mass

DY at 8 TeV

- ❖ MC@NLO: generate the hard process, while soft and collinear parts from NLO are subtracted.
- ❖ TMD adds those soft and collinear parts back.

- ❖ DY production very well described by
TMD with MC@NLO
- ❖ TMD with MC@NLO describes low q_T part
 - ❖ small uncertainties in small q_T region
 - ❖ **scale uncertainties** from hard process sizable!
- ❖ at larger q_T contribution from **DY+1 jet** significant.

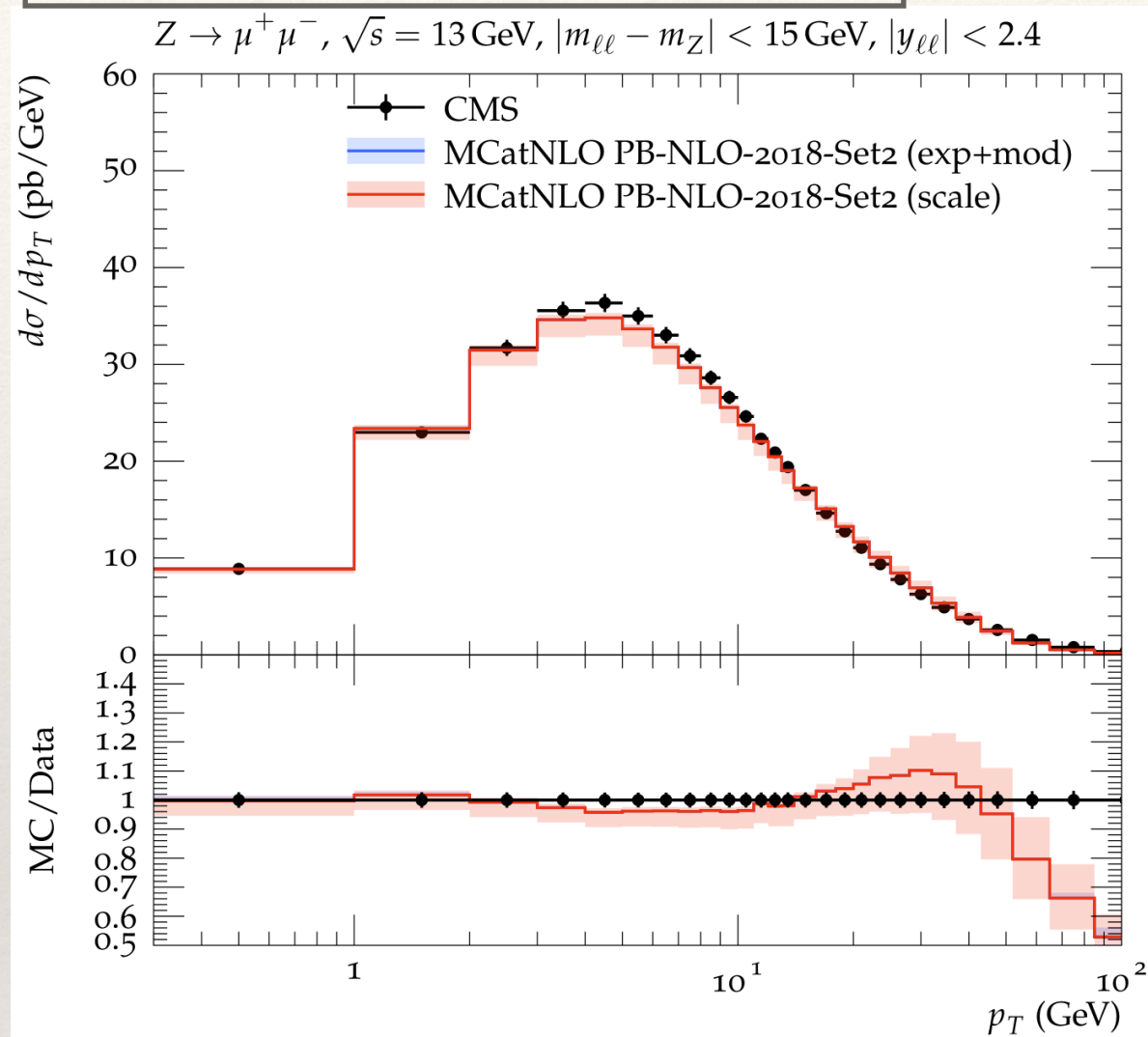
DY with PB TMD, Bermudez Martinez, A. et al,
PRD. 100.074027, arXiv:1906.00919



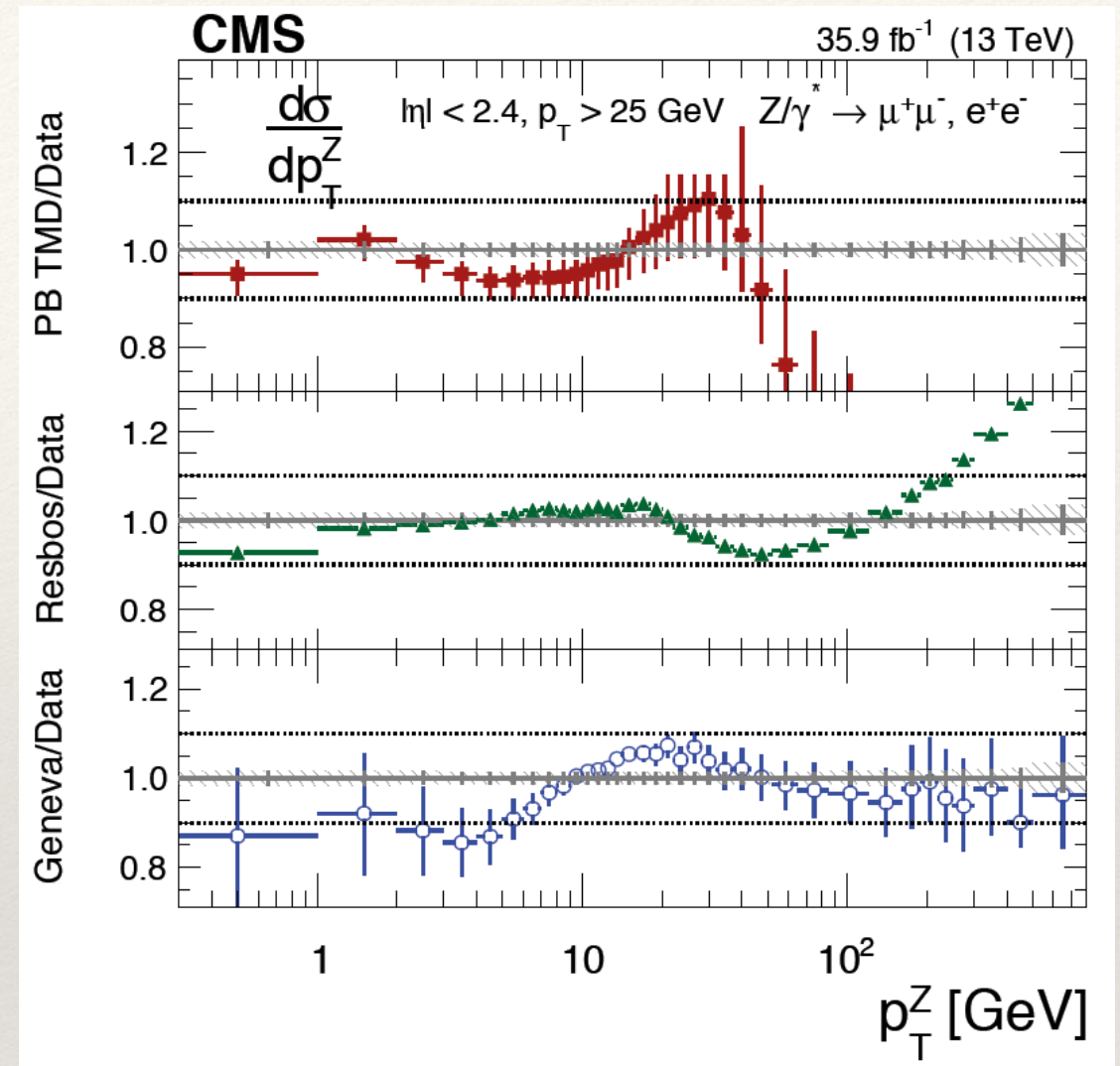
ATLAS (2016). DY at 8 TeV,
EPJC 76, 291, 1512.02192

DY at 13 TeV

Bermudez Martinez. A, et al, arXiv:2001.06488



SMP-17-010, JHEP12 (2019) 061



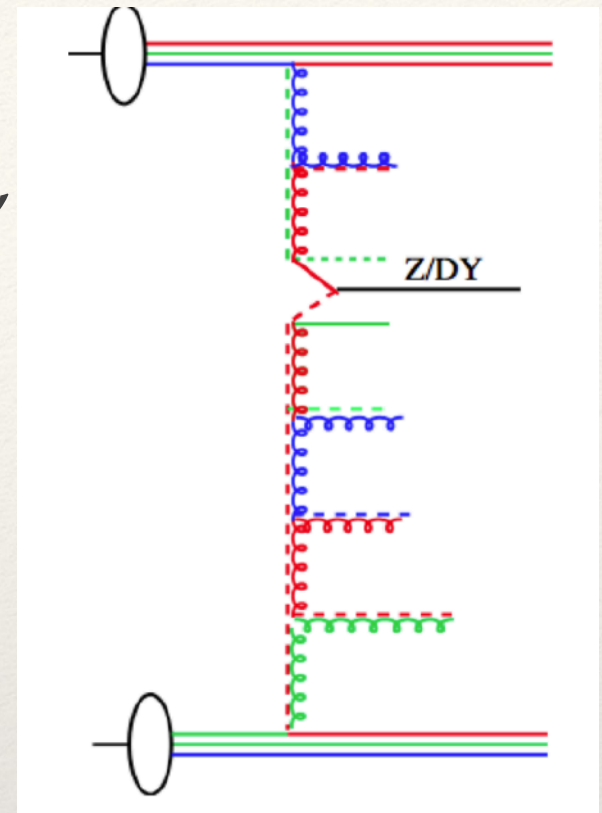
- ❖ Very good description of low p_T region
 - ❖ at large p_T contribution from higher order matrix elements important
- ❖ uncertainties in PB method mainly from scale of MC@NLO matrix element.

Application to Drell-Yan production

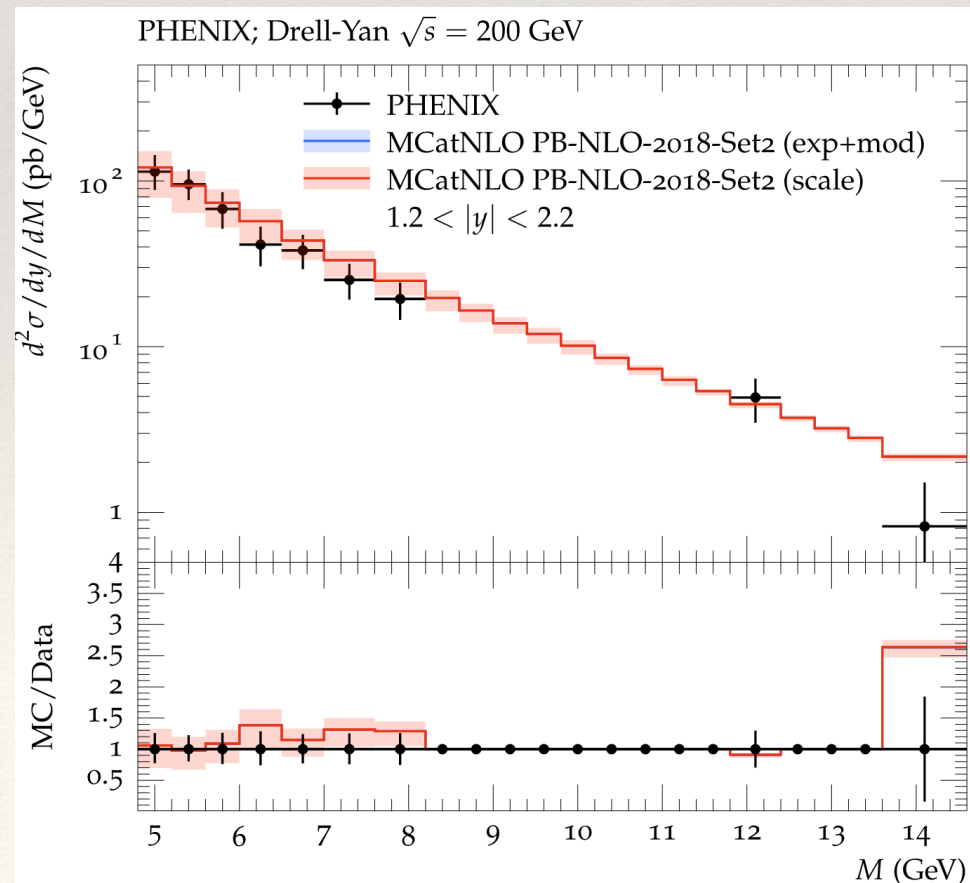
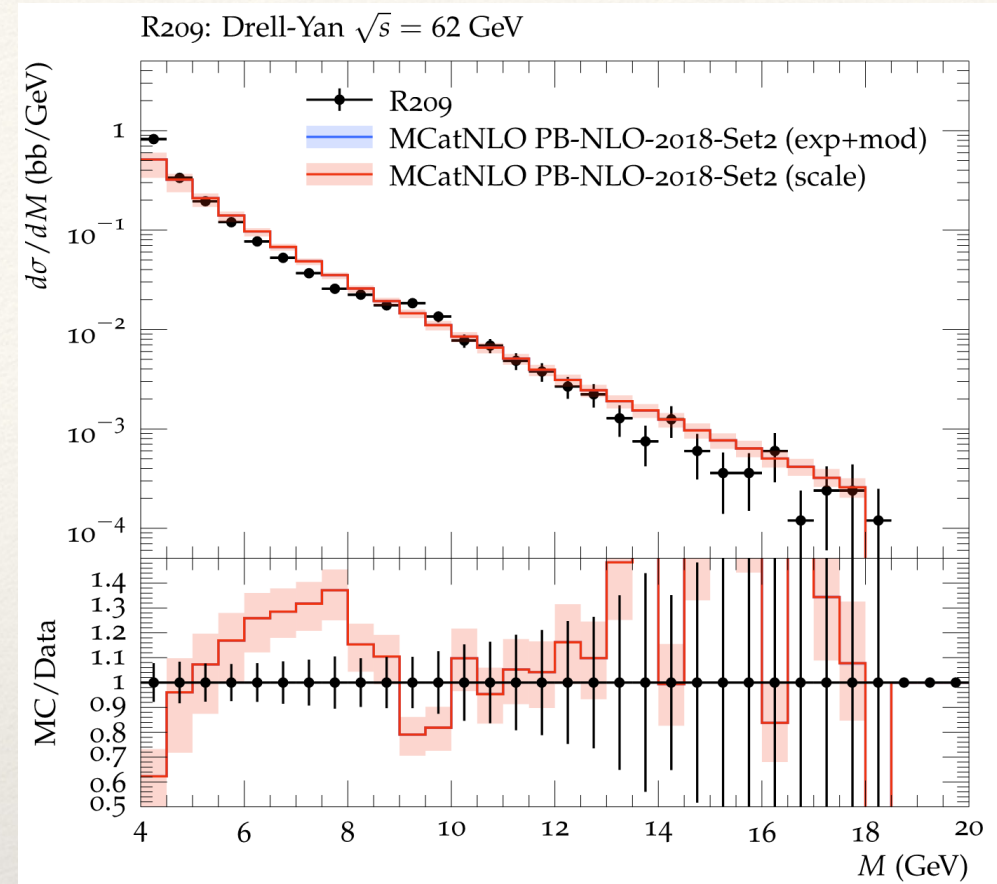
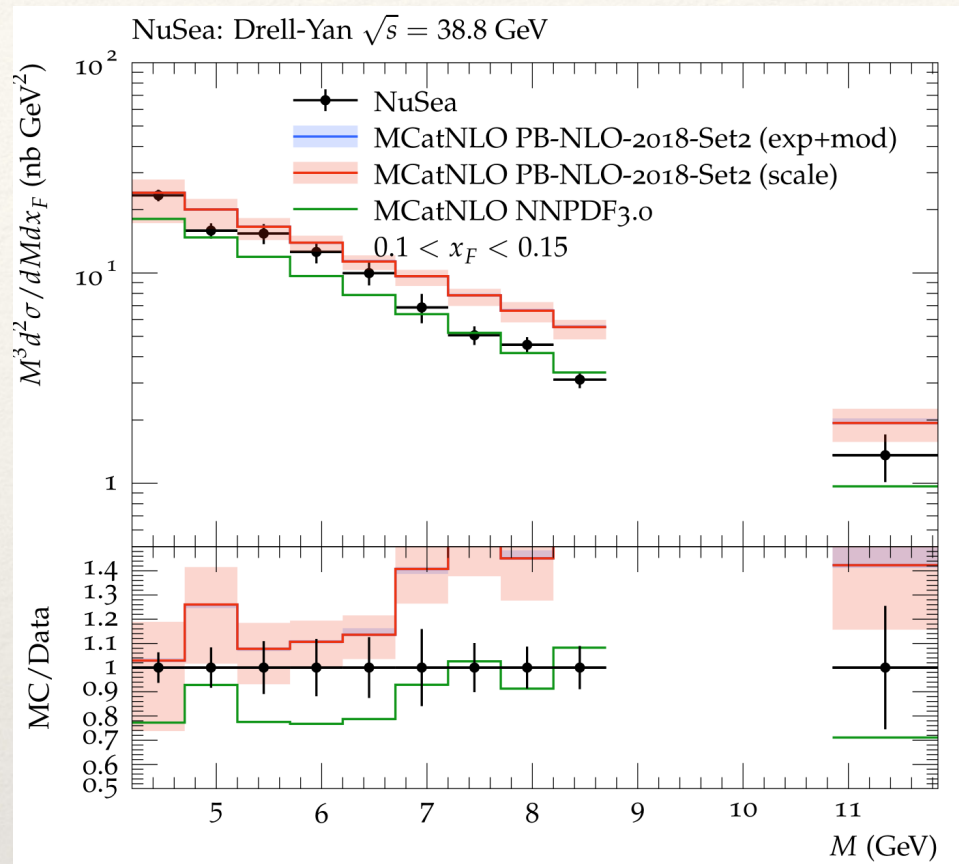
- ❖ Application in Drell-Yan (DY) production
 - ❖ DY production at LHC
 - ❖ **DY production at low mass and small \sqrt{s}**

DY at low mass and small \sqrt{s}

- ❖ at low mass, little room for QCD evolution
 - ❖ p_T of DY is dominated by intrinsic k_T and by soft gluons, which need to be resummed
- ❖ Latest measurement: PHENIX (PhysRevD. 99. 072003) at $\sqrt{s} = 200$ GeV for $4.8 \leq m_{DY} \leq 8.2$ GeV
- ❖ Other measurements (older)
 - ❖ R209 (1982) PhysRevLett. 48.302 at $\sqrt{s} = 62$ GeV (data read from plot in paper)
 - ❖ NUSEA (2003) hep-ex/0301031 at $\sqrt{s} = 38$ GeV (unpublished)
- ❖ Can PB method with MCatNLO be applied to small \sqrt{s} ?

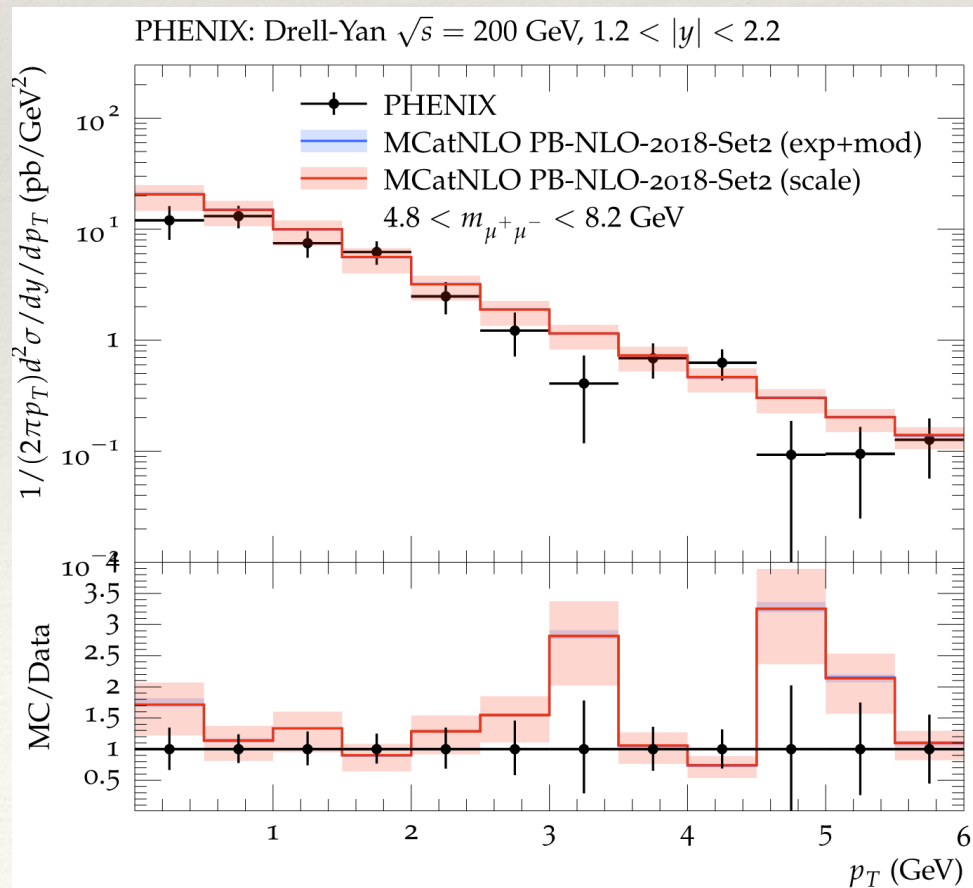
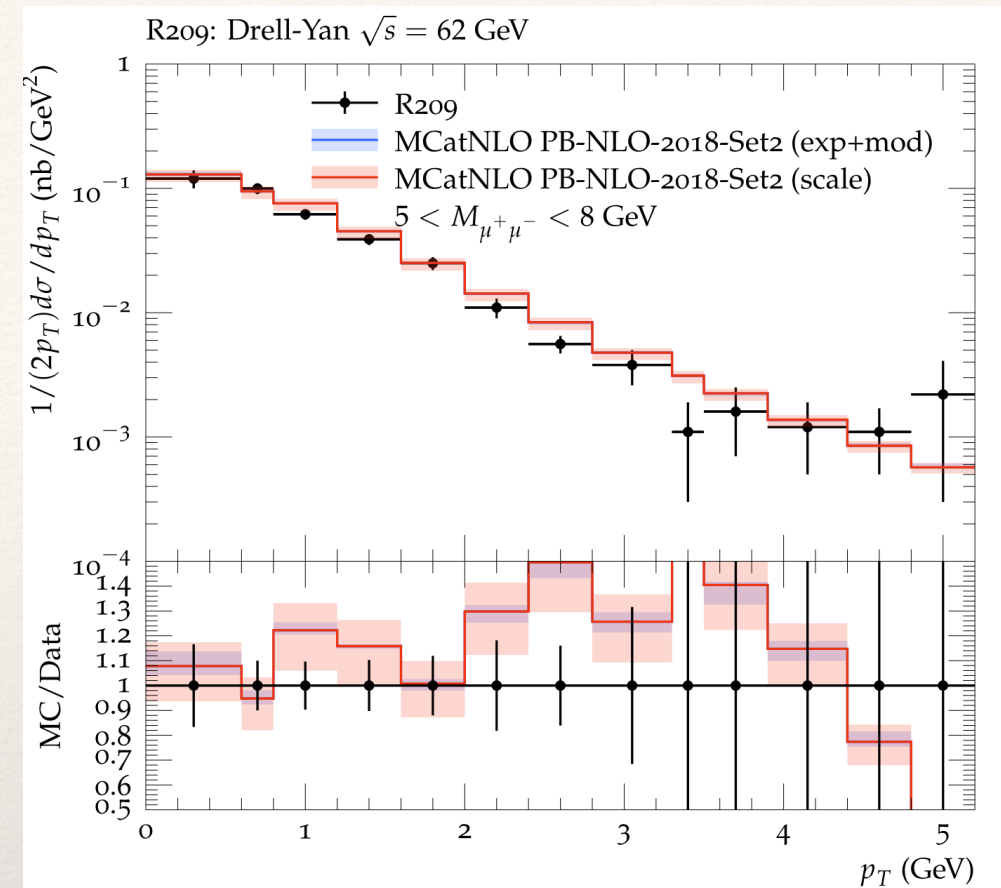
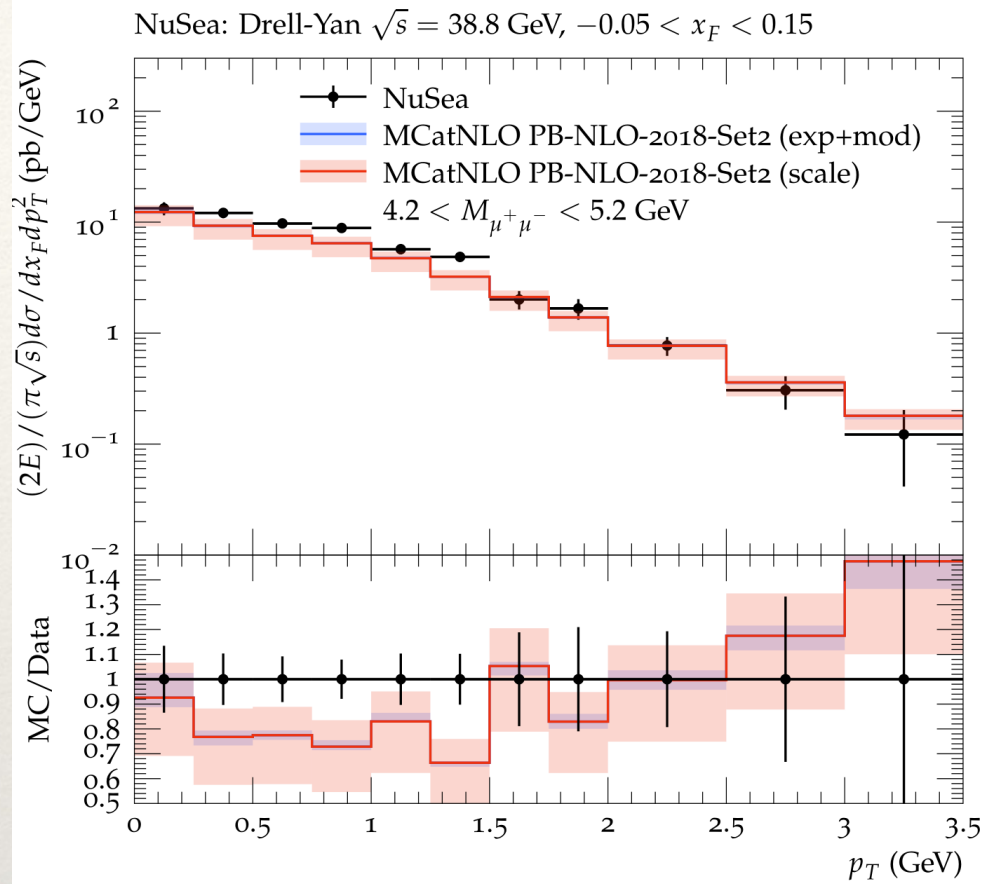


Comparison with measurements



- ❖ Mass distribution well described with PB pdfs
- ❖ Sensitive only to collinear pdf
 - ❖ At smallest \sqrt{s} , large x probed
 - ❖ Pdfs are fitted to HERA data and not well constrained at large x

DY pT spectrum



- ❖ DY pT spectrum well described with PB with MC@NLO
- ❖ Good agreement within uncertainties:

	NuSea	R209	PHENIX
χ^2/ndf	1.08	1.27	1.04

Conclusion

- ❖ Application to pp processes, DY:
 - ❖ DY q_T -spectrum without new parameters
 - ❖ Agree well with results from LHC at low p_T
 - ❖ DY q_T -spectrum at low mass and low energies well described
 - ❖ Success of PB TMDs with MC@NLO:
 - ❖ Describe DY production over wide range
 - ❖ Proper prediction of low p_T spectrum-needed for $m(W)$ determination

Backup

Thank you for your attention!

DGLAP evolution-solution with Parton branching method

- ❖ DGLAP evolution in differential form

$$\mu^2 \frac{\partial}{\partial \mu^2} f(x, \mu^2) = \int \frac{dz}{z} \frac{\alpha_s}{2\pi} P^{(R)}(z) f\left(\frac{x}{z}, \mu^2\right)$$

- ❖ Sudakov form factor:

$$\Delta_s(\mu^2) = \exp\left(-\int^{z_M} dz \int_{\mu_0^2}^{\mu^2} \frac{\alpha_s}{2\pi} \frac{d\mu'^2}{\mu'^2} P^{(R)}(z)\right)$$

- ❖ introduce Sudakov form factor:

$$\mu^2 \frac{\partial}{\partial \mu^2} \frac{f(x, \mu^2)}{\Delta_s(\mu^2)} = \int \frac{dz}{z} \frac{\alpha_s}{2\pi} \frac{P^{(R)}(z)}{\Delta_s(\mu^2)} f\left(\frac{x}{z}, \mu^2\right)$$

- ❖ Then one obtains its integral form:

$$\mathbf{f}(\mathbf{x}, \mu^2) = f(x, \mu_0^2) \Delta_s(\mu^2) + \int_x^{z_M} \frac{dz}{z} \int_{\mu_0^2}^{\mu^2} \frac{d\mu'^2}{\mu'^2} \frac{\Delta_s(\mu^2)}{\Delta_s(\mu'^2)} P^{(R)}(z) \mathbf{f}\left(\frac{\mathbf{x}}{z}, \mu'^2\right)$$

No-branching probability from μ_0^2 to μ^2

PB: Iterative solution

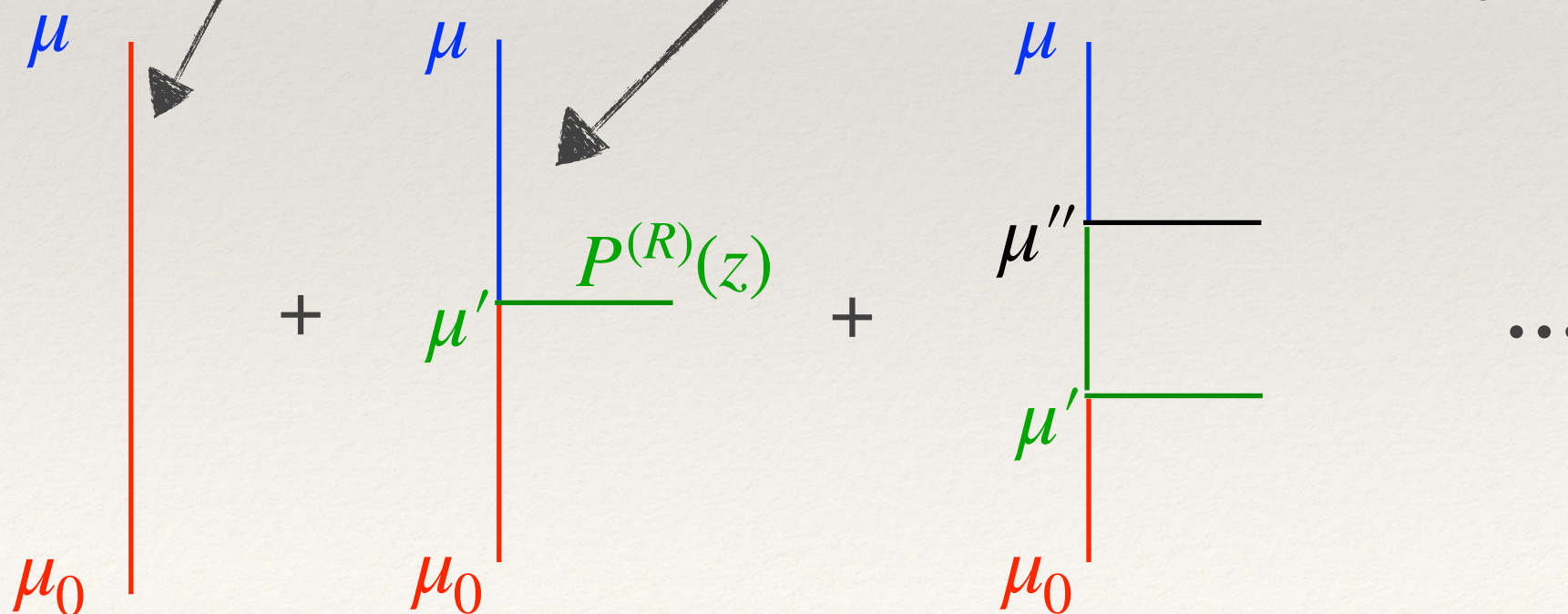
$$\mathbf{f}(\mathbf{x}, \mu^2) = f(x, \mu_0^2) \Delta_s(\mu^2) + \int_x^{z_M} \frac{dz}{z} \int_{\mu_0^2}^{\mu^2} \frac{d\mu'^2}{\mu'^2} \frac{\Delta_s(\mu'^2)}{\Delta_s(\mu'^2)} P^{(R)}(z) \mathbf{f}\left(\frac{\mathbf{x}}{z}, \mu'^2\right)$$

- ❖ Solve integral equation via iteration:

$$\mathbf{f}_0(\mathbf{x}, \mu^2) = f(x, \mu_0^2) \Delta(\mu^2)$$

$$\mathbf{f}_1(\mathbf{x}, \mu^2) = f(x, \mu_0^2) \Delta(\mu^2) + \int_{\mu_0^2}^{\mu^2} \frac{d\mu'^2}{\mu'^2} \frac{\Delta(\mu'^2)}{\Delta(\mu'^2)} \int_x^{z_M} \frac{dz}{z} P^{(R)}(z) \underbrace{\mathbf{f}\left(\frac{\mathbf{x}}{z}, \mu_0^2\right) \Delta(\mu'^2)}_{f_0}$$

$$\mathbf{f}_2(\mathbf{x}, \mu^2) = \dots$$



Transverse Momentum Dependence

- ❖ Parton Branching evolution generates every single branching:
 - ❖ Kinematics can be calculated at every step

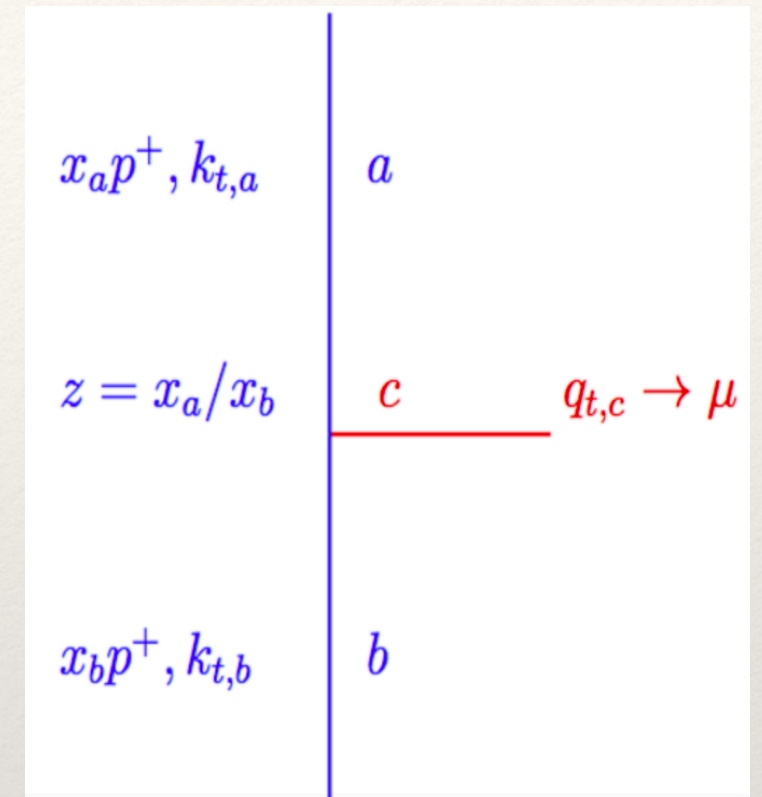
- ❖ Give physics interpretation of evolution scale:

- ❖ p_T -ordering:

$$\mu = q_T$$

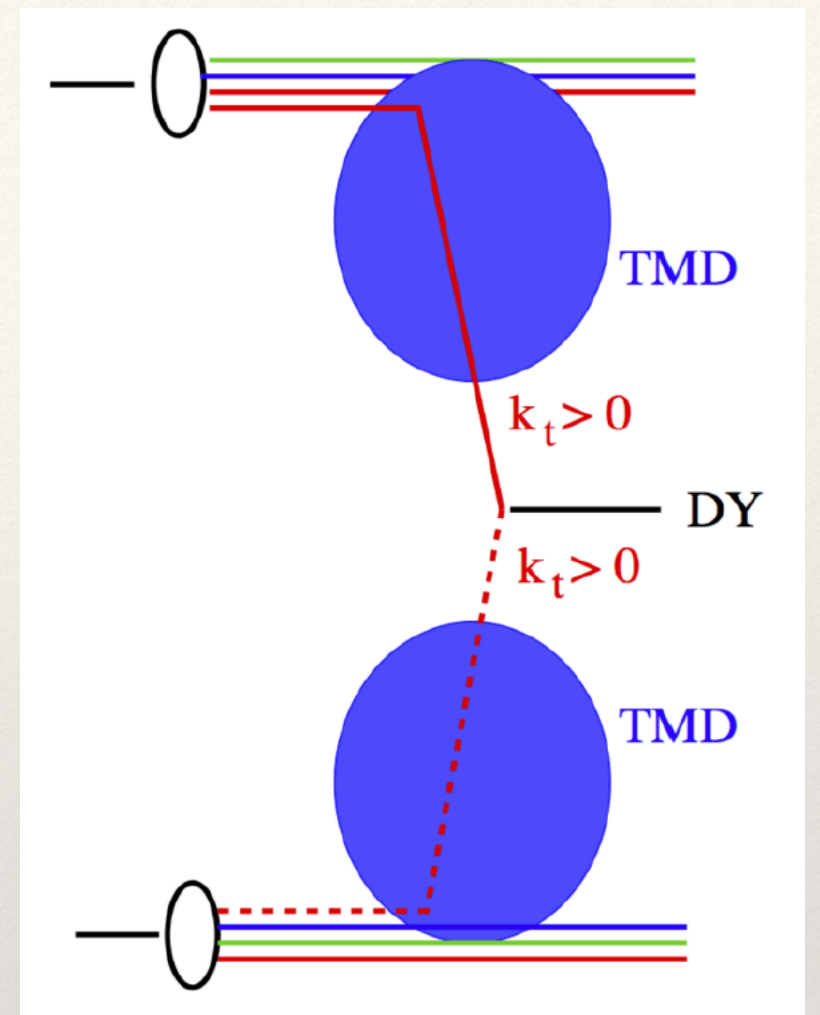
- ❖ Angular ordering:

$$\mu = q_T/(1 - z)$$



Drell-Yan production: qT spectrum

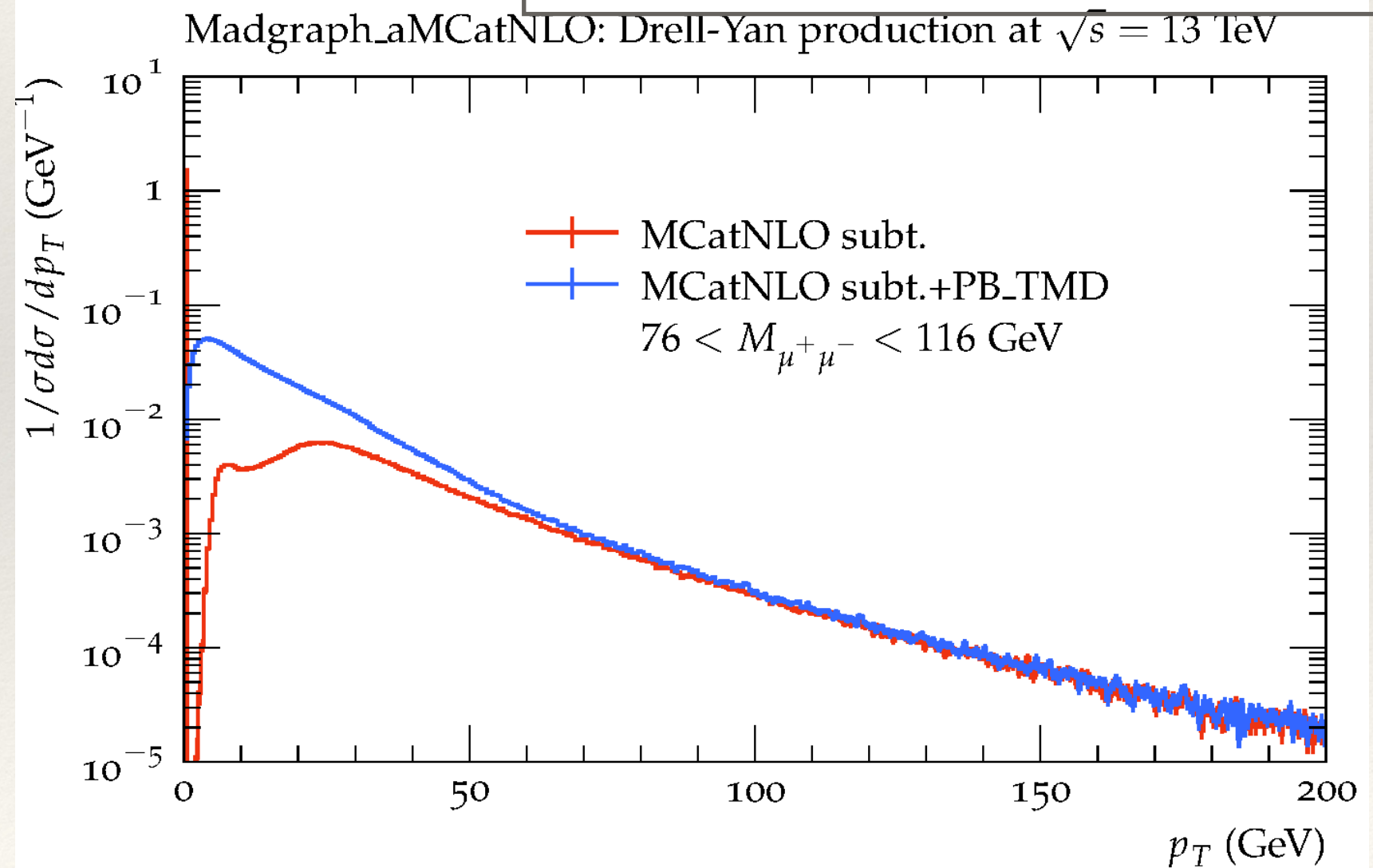
- ❖ Drell-Yan (DY) production
 - ❖ $q\bar{q} \rightarrow Z_0$
 - ❖ add k_T for each parton as function of k_T and μ according to TMD
 - ❖ Keep final state mass fixed:
 - ❖ x_1 and x_2 (light-cone fraction) are different after adding k_T



Matching to hard process: MC@NLO method

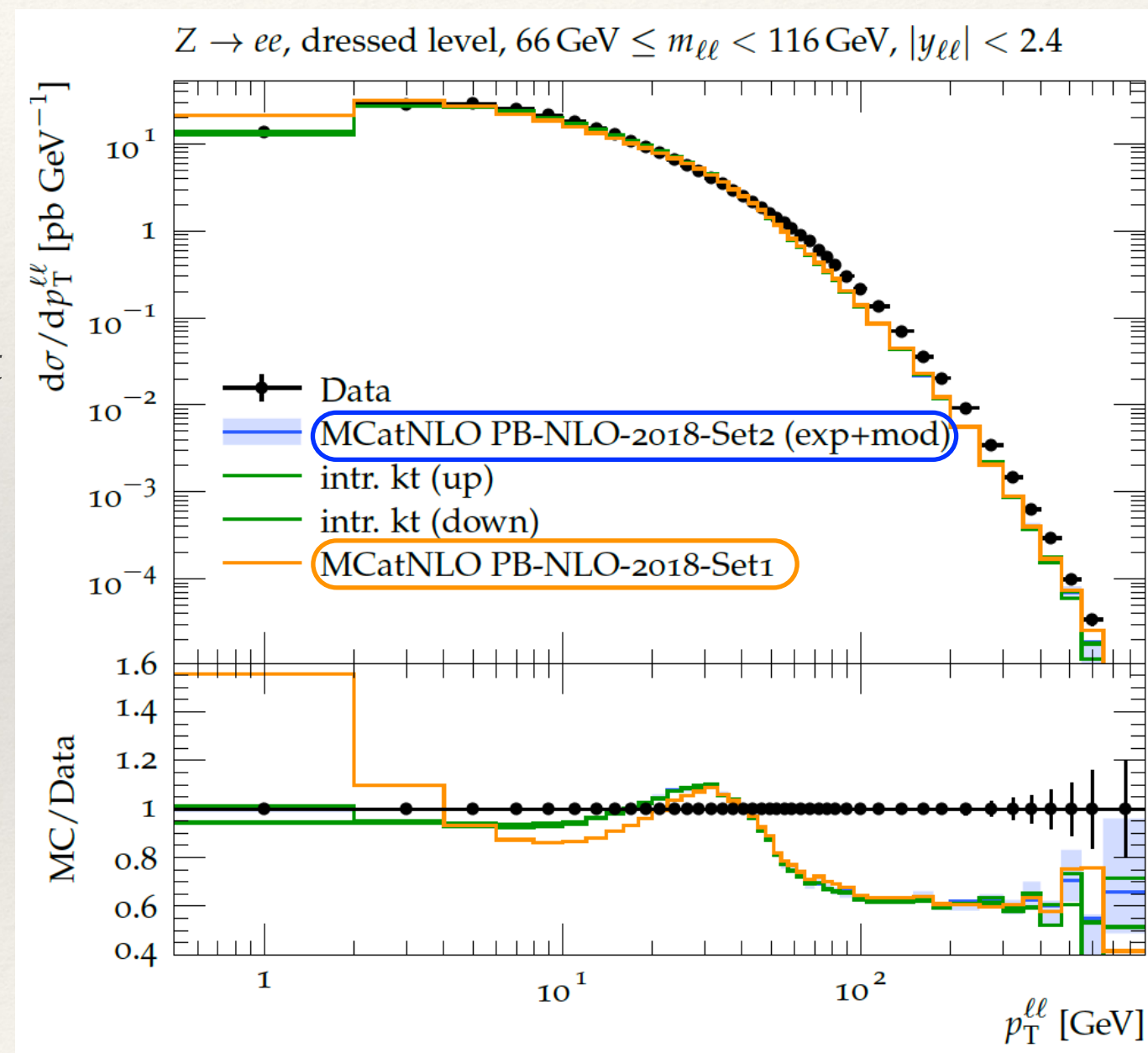
- ❖ MC@NLO: soft and collinear parts from NLO are subtracted, that can be added back by TMD or parton shower later.
- ❖ MC@NLO without shower unphysical
 - ❖ use herwig6 subtraction terms
- ❖ low q_T region affected by subtraction of Soft & collinear parts

The transverse momentum spectrum of low mass Drell-Yan production at next-to-leading order in the Parton Branching method, Bermudez Martinez, A, et al, arXiv:2001.06488



Z-boson production at 8 TeV

- ❖ Z-boson production at 8 TeV ATLAS is compared with prediction MC@NLO with PB-TMD.
- ❖ Predictions using PB-2018-Set1 ($\alpha_s(q)$) and Set2 ($\alpha_s(q(1-z))$) parton distributions:
 - ❖ Set1 overshoots the measurements at small q_T .
 - ❖ Set2 agrees well with measurement.
- ❖ The deviation at higher q_T comes from missing higher order contributions in the matrix element calculation.



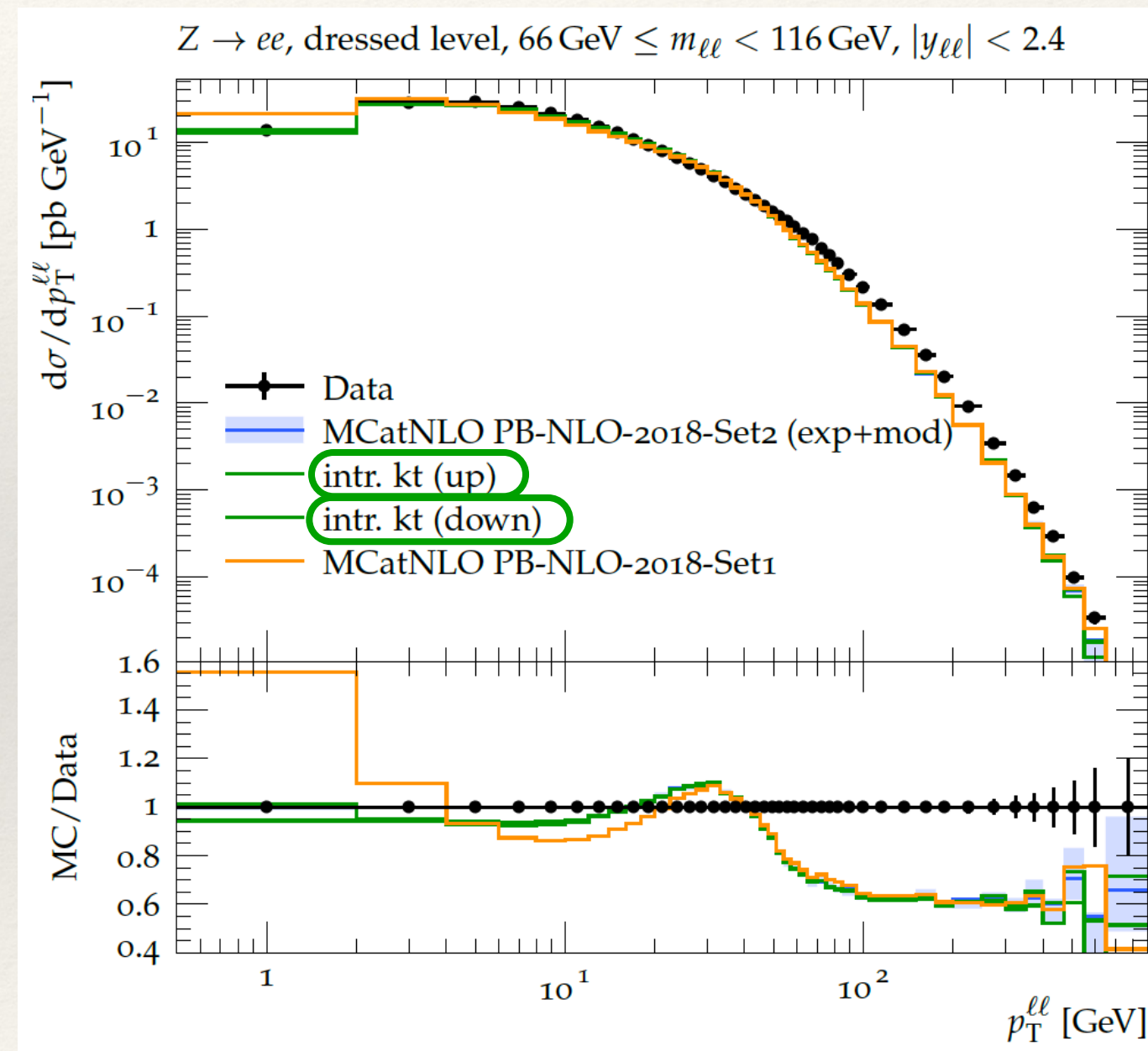
ATLAS (2016). DY at 8 TeV, EPJC 76, 291, 1512.02192

Z-boson production at 8TeV

❖ Z-boson production at 8 TeV ATLAS is compared with prediction MC@NLO with PB-TMD.

❖ Predictions using PB-2018-Set1 ($\alpha_s(q)$) and Set2 ($\alpha_s(q(1-z))$) parton distributions.

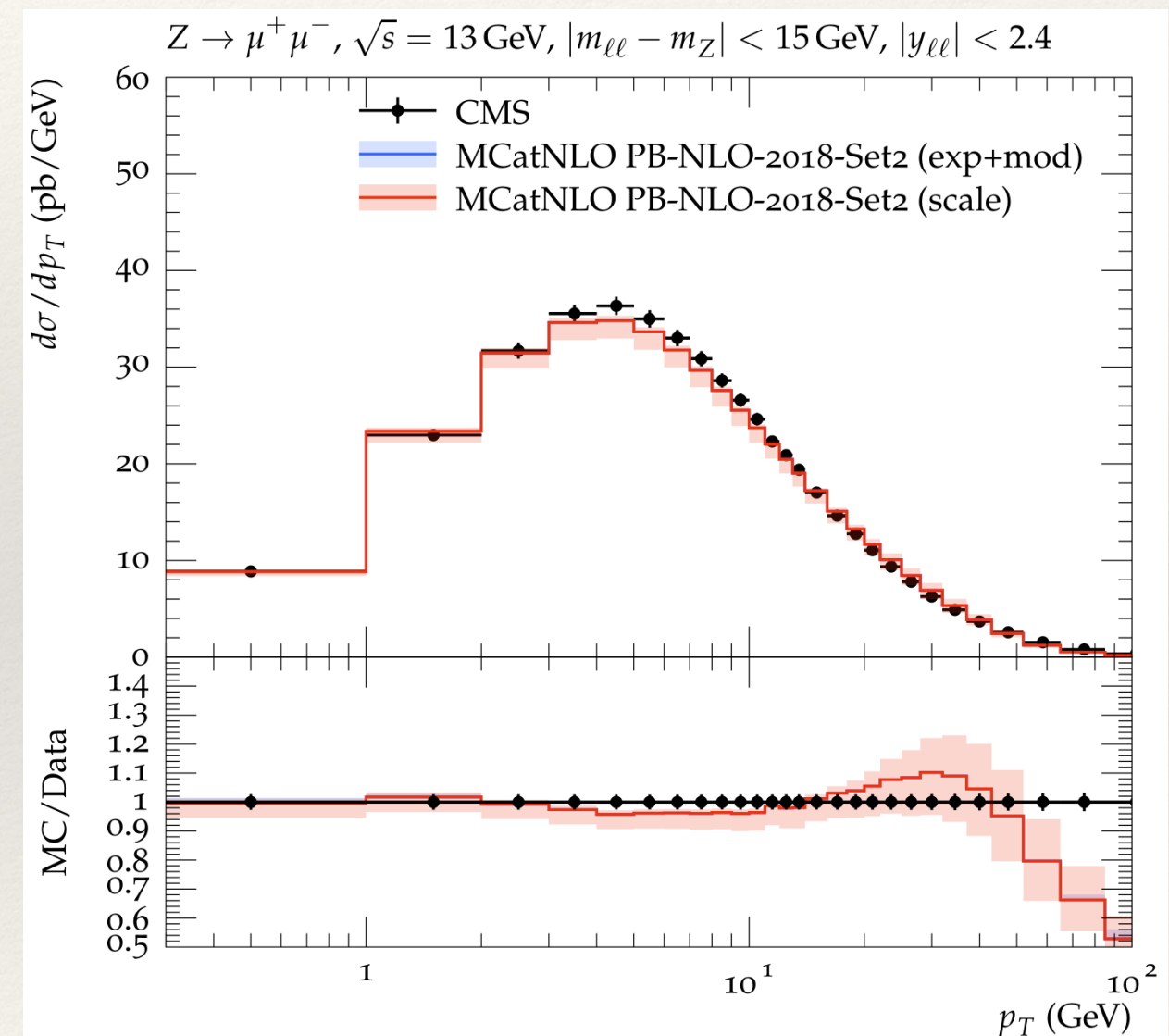
❖ Varying the mean of intrinsic kt distribution by factor 2, small



ATLAS (2016). DY at 8 TeV, EPJC 76, 291, 1512.02192

Z-boson production at 13 TeV

- ❖ Z-boson production at 13 TeV CMS is compared with prediction MC@NLO with PB-TMD.
- ❖ The prediction agrees well with the measurement in the low p_T region,
- ❖ but deviates at high p_T because of missing Z+jets matrix element calculation.
- ❖ The dominate theory uncertainties are from scale of MC@NLO matrix element.

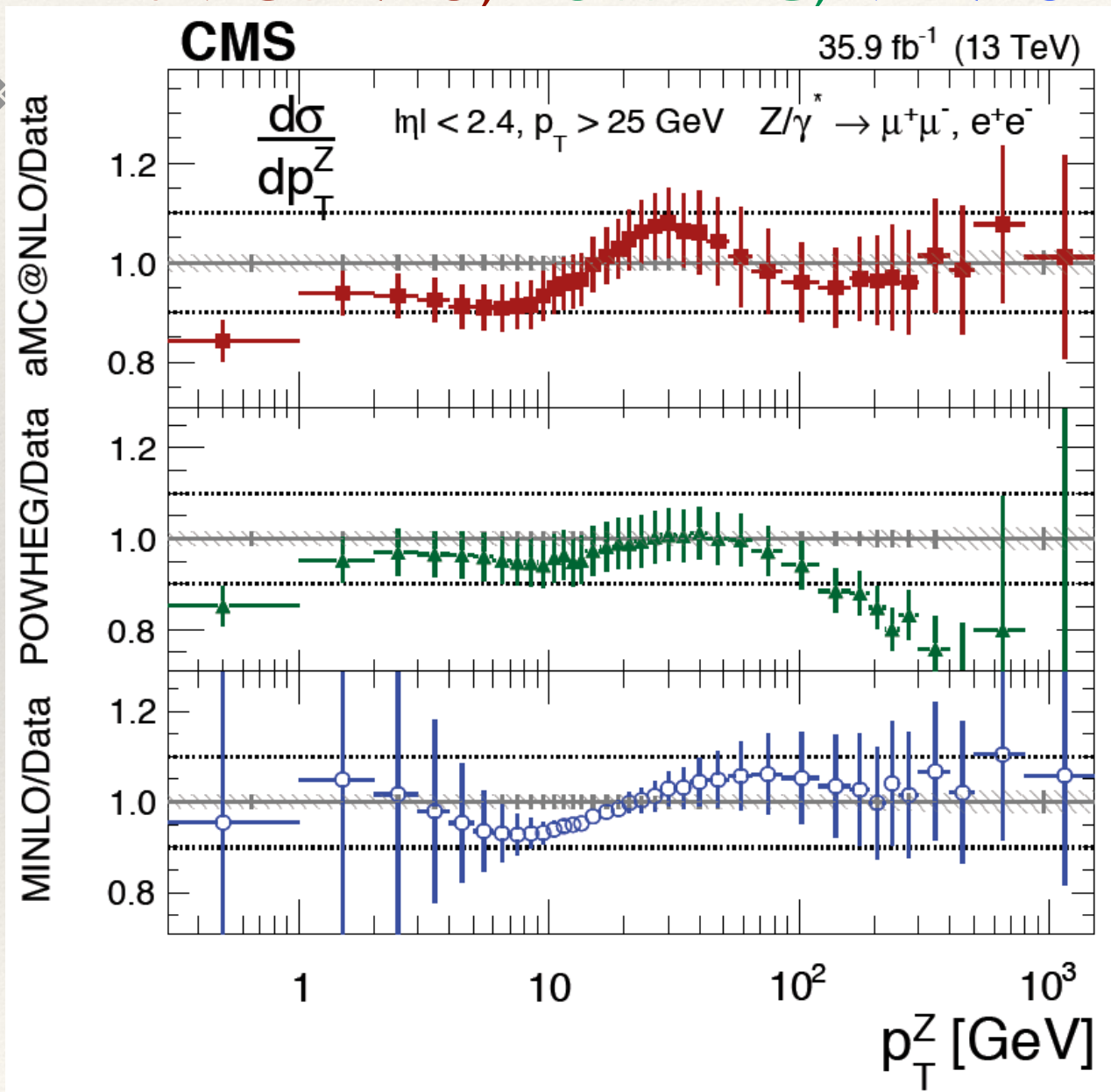


CMS (2016). DY at 13 TeV, submitted, 1909.04133

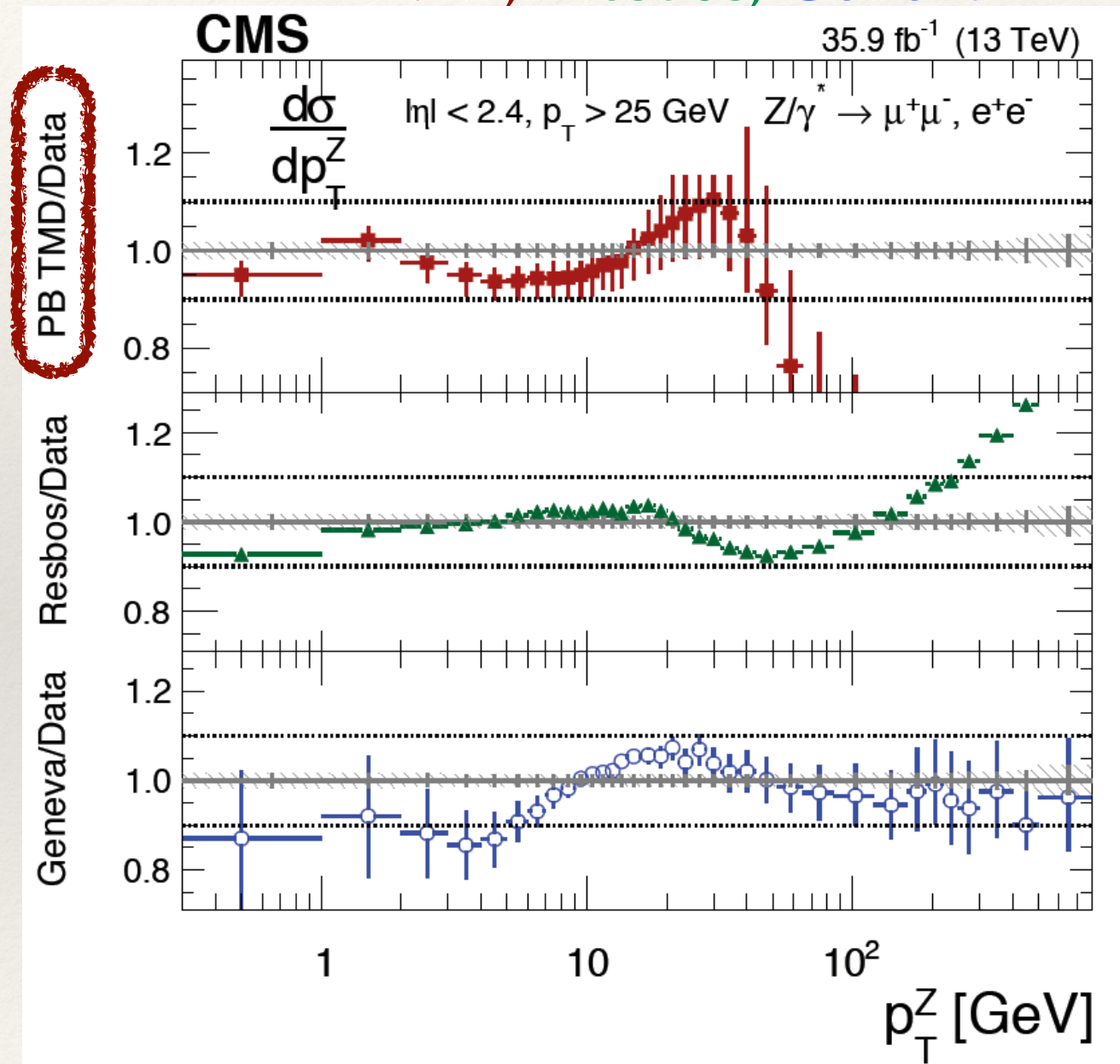
Z-boson production at 13 TeV

- Z-boson production at 13 TeV CMS is compared with predictions **MC@NLO** with **PB-TMD**.

aMC@NLO, POWHEG, MINLO



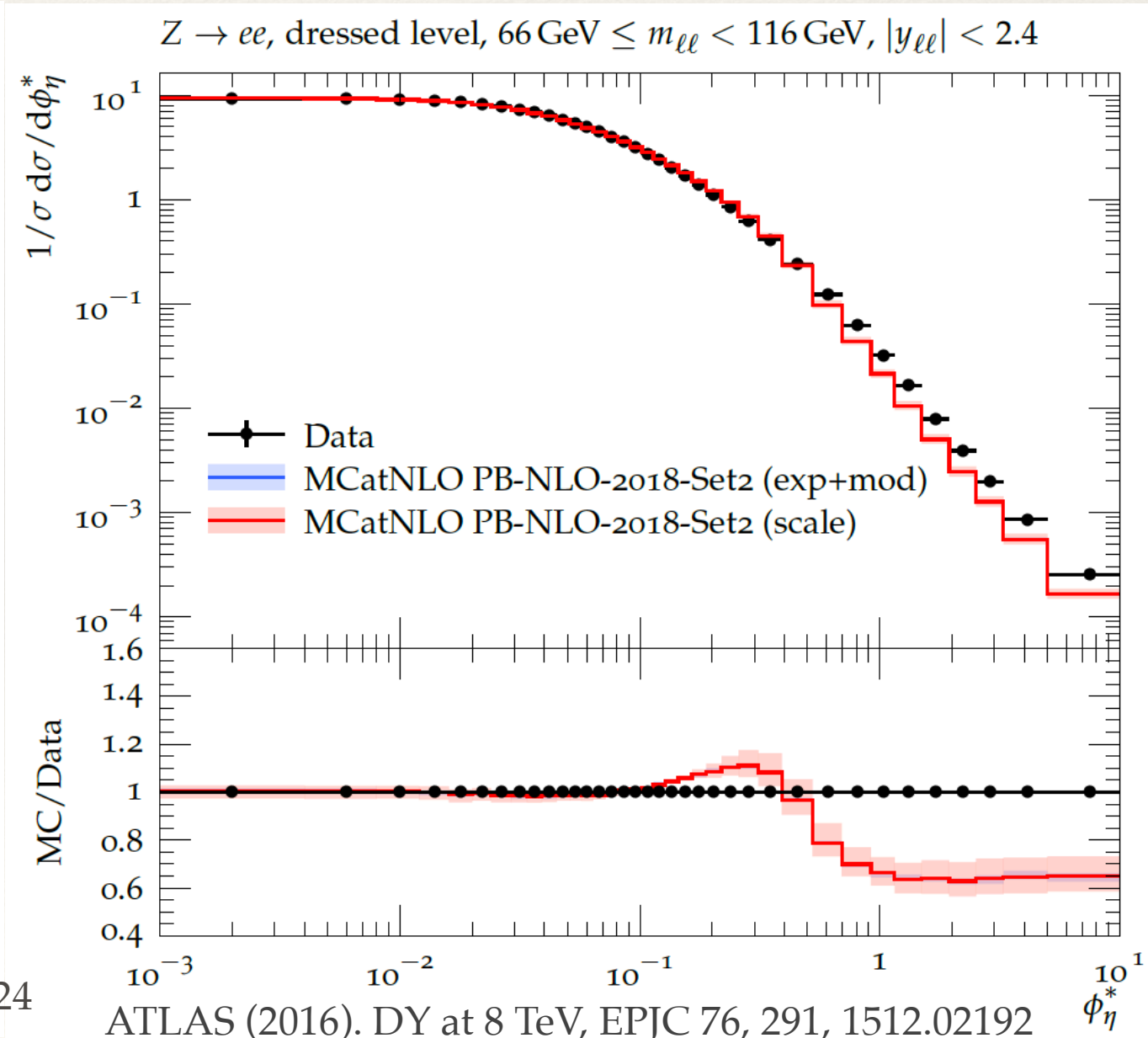
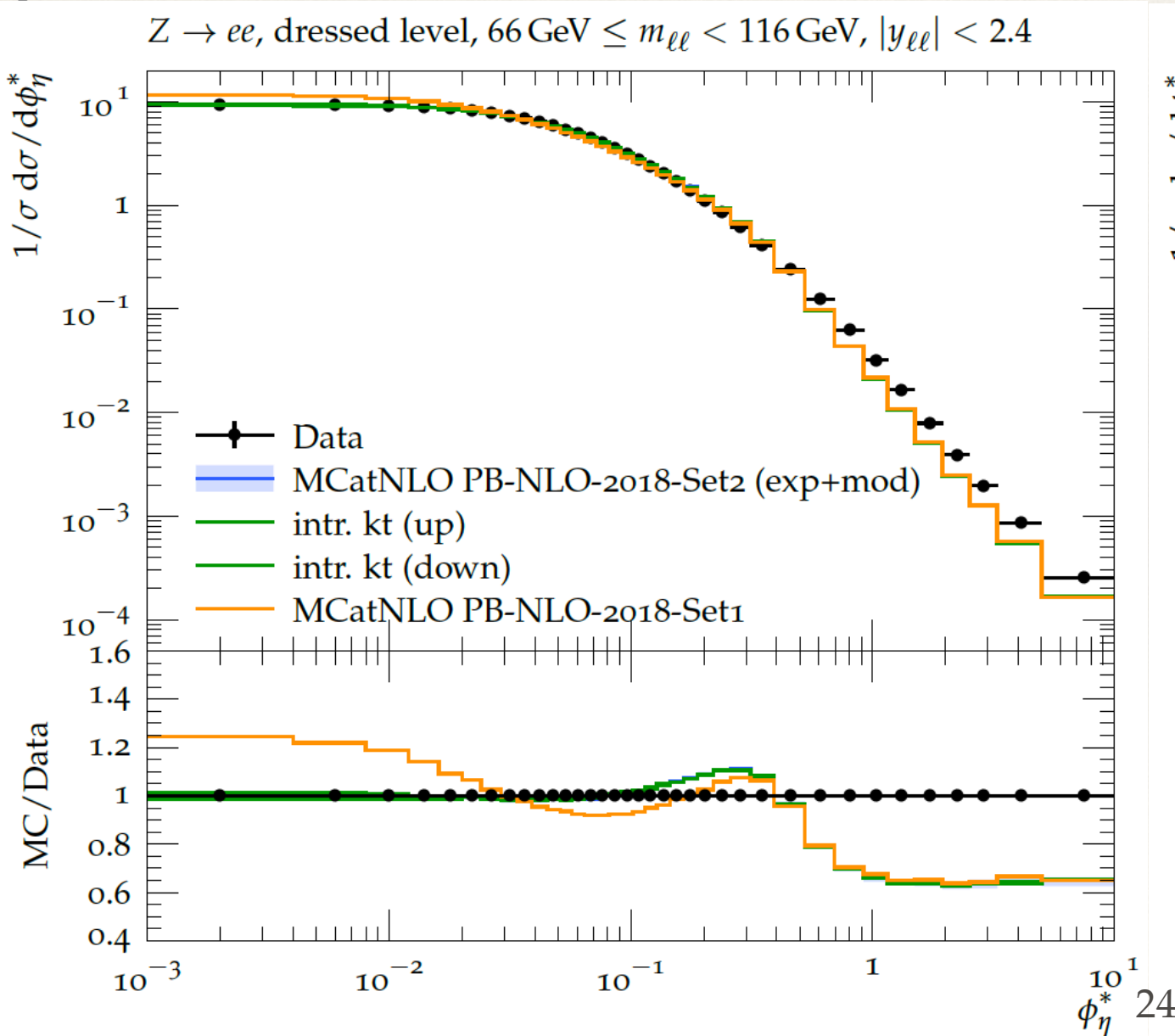
PB-TMD, Resbos, Geneva



- The PB TMD prediction describes data well at low p_T .

Z-boson production at 8 TeV

- ❖ Z-boson production at 8 TeV ATLAS is compared with prediction **MC@NLO with PB-TMD**.
- ❖ The ϕ^* distribution are compared also.



Difficulties at small q_T and small \sqrt{s}

PHYSICAL REVIEW D **100**, 014018 (2019)

Difficulties in the description of Drell-Yan processes at moderate invariant mass and high transverse momentum

Alessandro Bacchetta,^{1,2,*} Giuseppe Bozzi,^{1,2,†} Martin Lambertsen,^{3,‡} Fulvio Piacenza,^{1,2,§}
Julius Steiglechner,^{3,||} and Werner Vogelsang^{3,¶}

¹*Dipartimento di Fisica, Università di Pavia, via Bassi 6, I-27100 Pavia, Italy*

²*INFN Sezione di Pavia, via Bassi 6, I-27100 Pavia, Italy*

³*Institute for Theoretical Physics, Tübingen University, Auf der Morgenstelle 14, D-72076 Tübingen, Germany*



(Received 30 January 2019; published 22 July 2019)

Both regimes, $q_T \ll Q$ and $q_T \sim Q$, as well as their matching, must be under theoretical control in order to have a proper understanding of the physics of the Drell-Yan process. In the present work, we study the process at fixed-target energies for moderate values of the invariant mass Q and in the region $q_T \lesssim Q$. We focus on the predictions based on collinear factorization and examine their ability to describe the experimental data in this regime. We find, in fact, that the predicted cross sections fall significantly short of the available data even at the highest accessible values of q_T . We investigate possible sources of uncertainty in the predictions based on collinear factorization, and two extensions of the collinear framework: the resummation of high- q_T threshold logarithms, and transverse-momentum smearing. None of these appear to lead to a satisfactory agreement with the data. We argue that these findings also imply that the Drell-Yan cross section in the “matching regime” $q_T \lesssim Q$ is presently not fully understood at fixed-target energies.

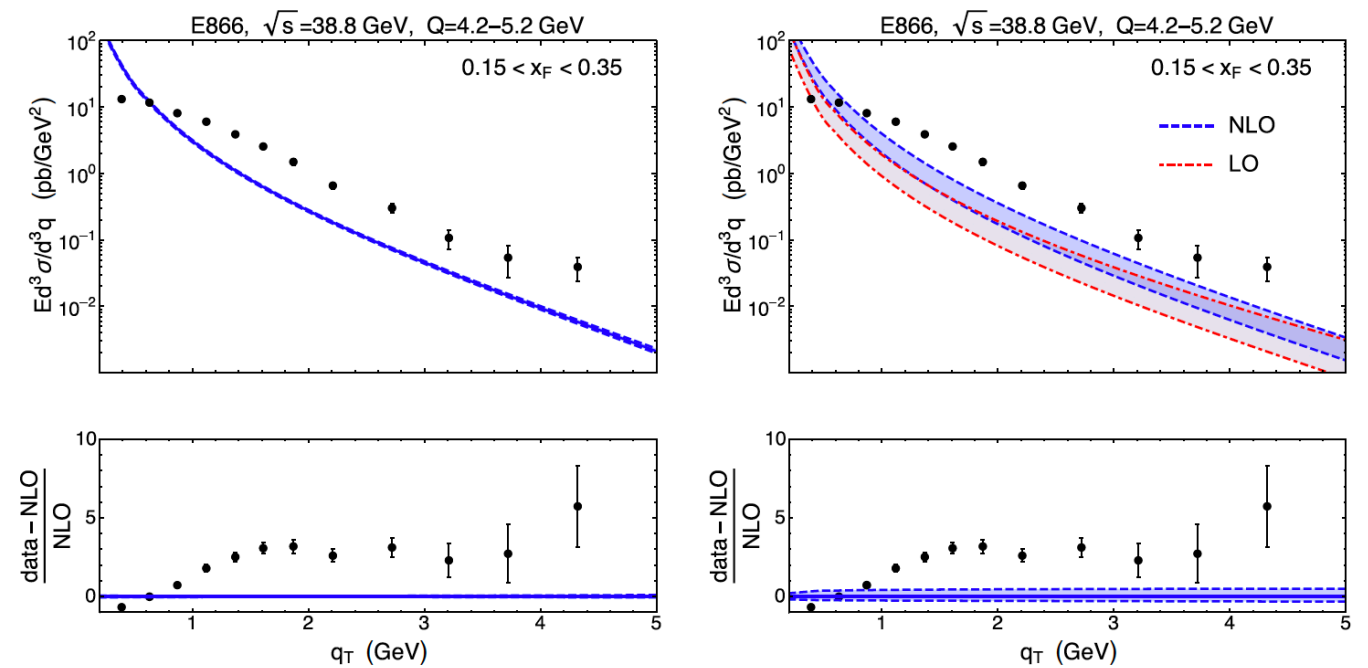
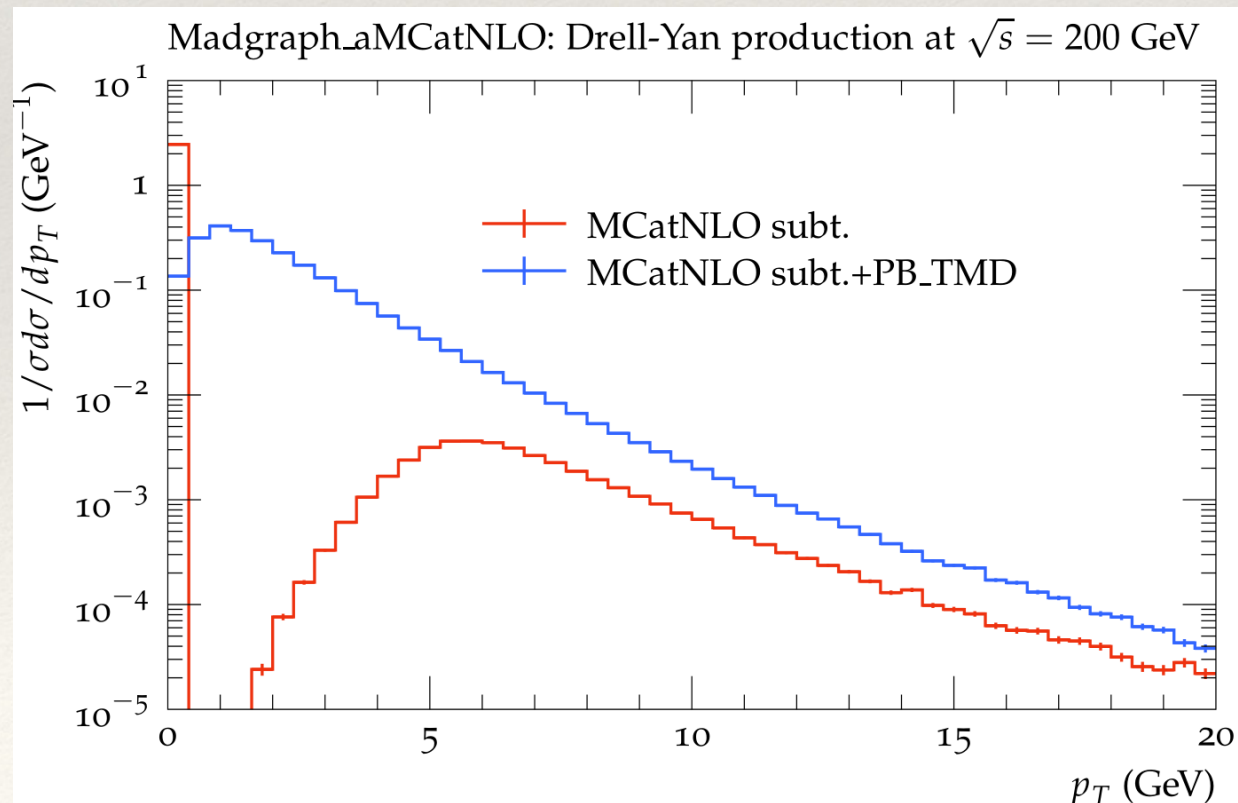
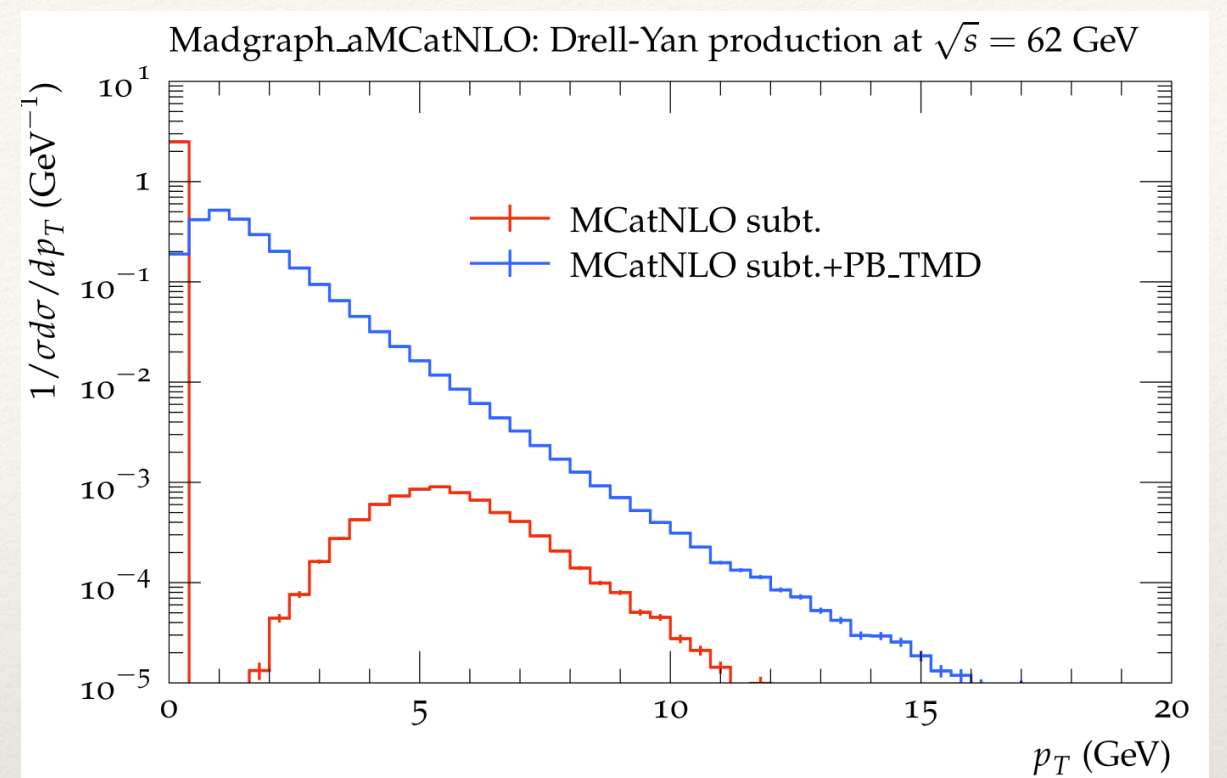
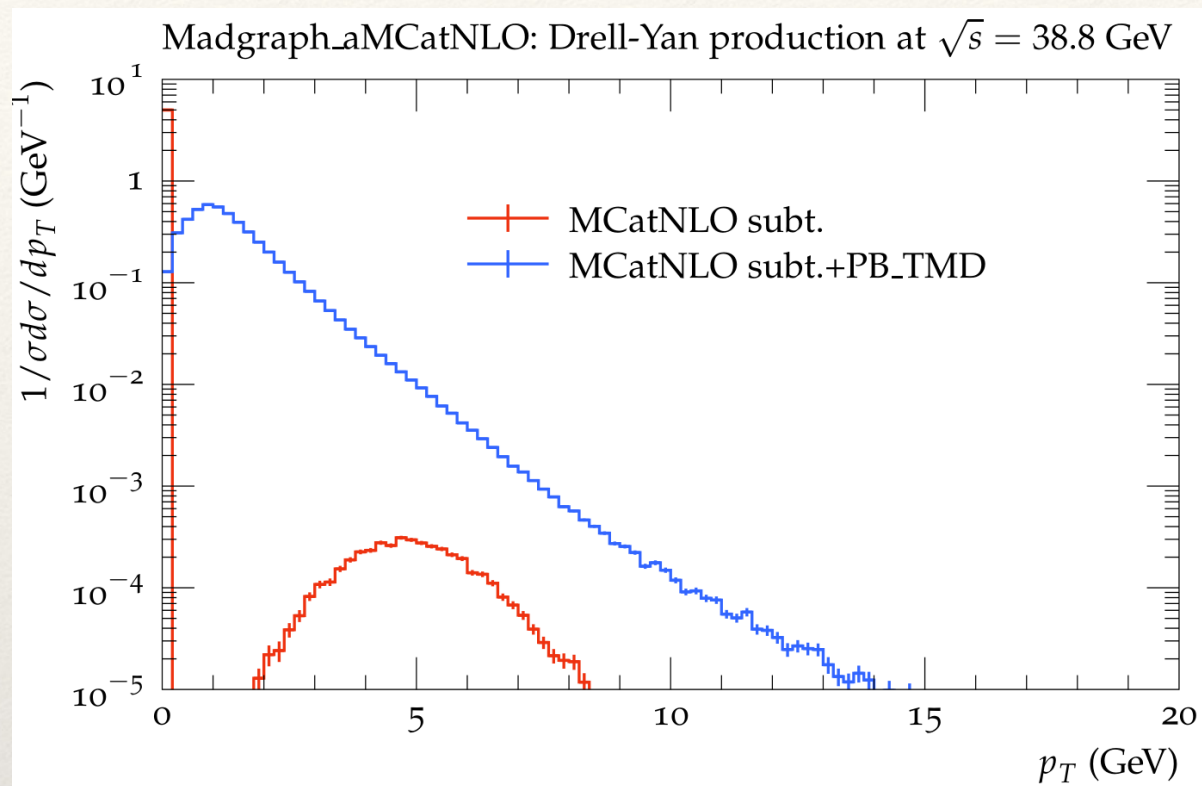


FIG. 2. Transverse-momentum distribution of Drell-Yan dimuon pairs at $\sqrt{s} = 38.8$ GeV in a selected invariant mass range and Feynman- x range: experimental data from Fermilab E866 (hydrogen target) [41] compared to LO QCD and NLO QCD results. (Left panels) NLO QCD [$\mathcal{O}(\alpha_s^2)$] calculation with central values of the scales $\mu_R = \mu_F = Q = 4.7$ GeV, including a 90% confidence interval from the CT14 PDF set [39]. (Right panels) LO QCD and NLO QCD theoretical uncertainty bands obtained by varying the renormalization and factorization scales independently in the range $Q/2 < \mu_R, \mu_F < 2Q$.

DY at low mass and small \sqrt{s}



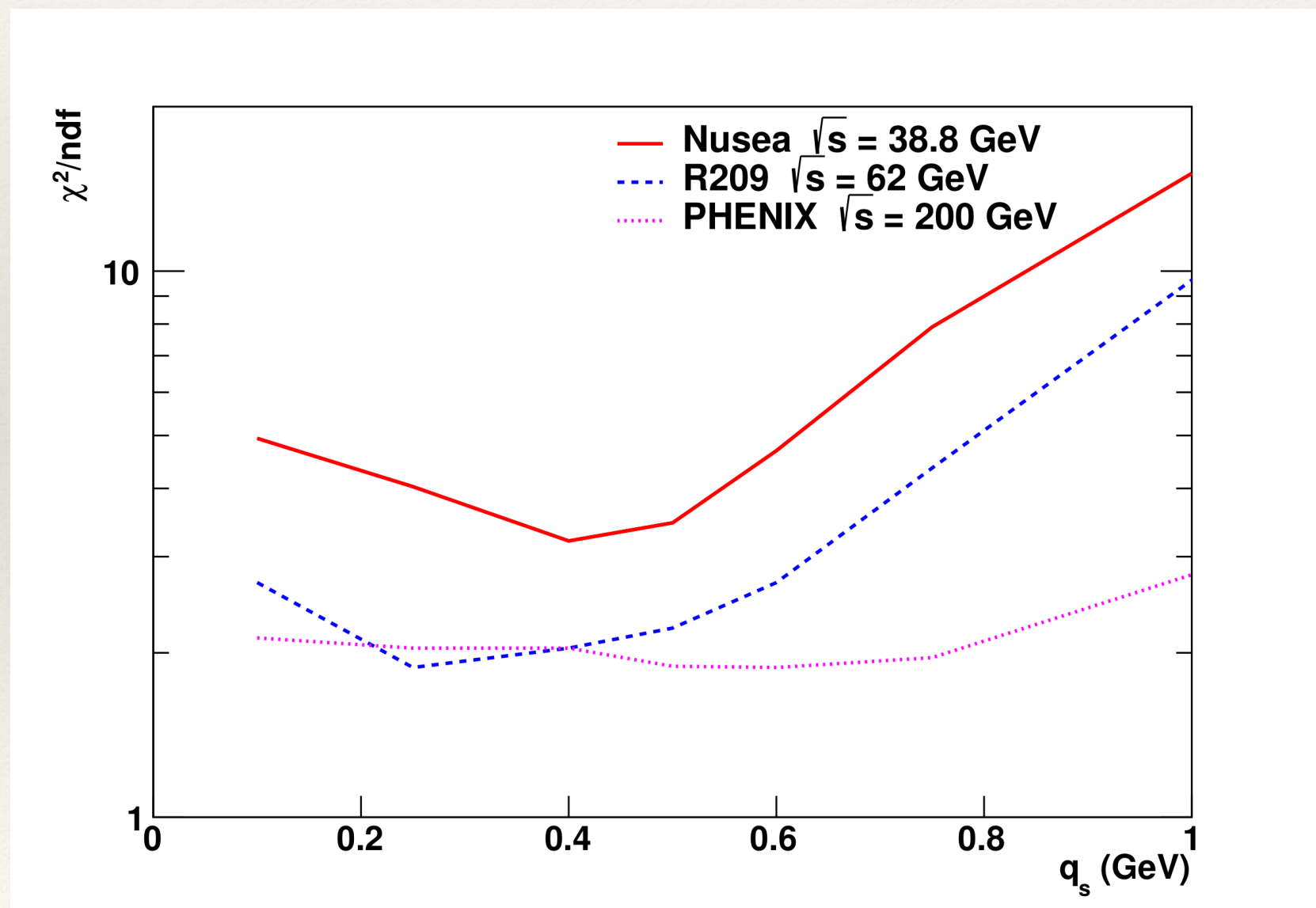
- ❖ Contribution of real 1 parton emission increases with \sqrt{s}
- ❖ NLO corrections are large at small m_{DY} (factor of 2 or more) because scale (m_{DY}) is small and $\alpha_s(m_{DY})$ is large!

Constraints on intrinsic kT

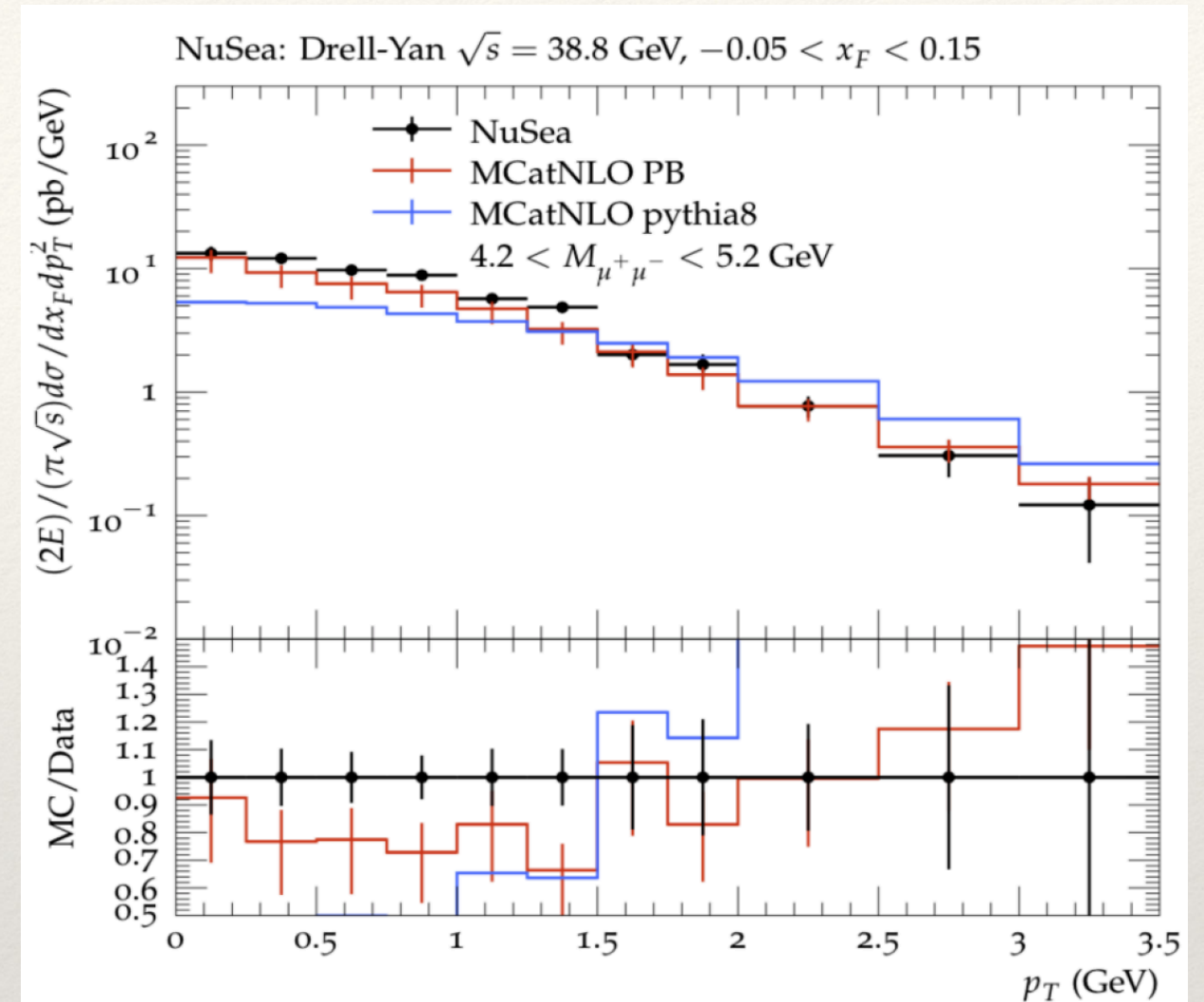
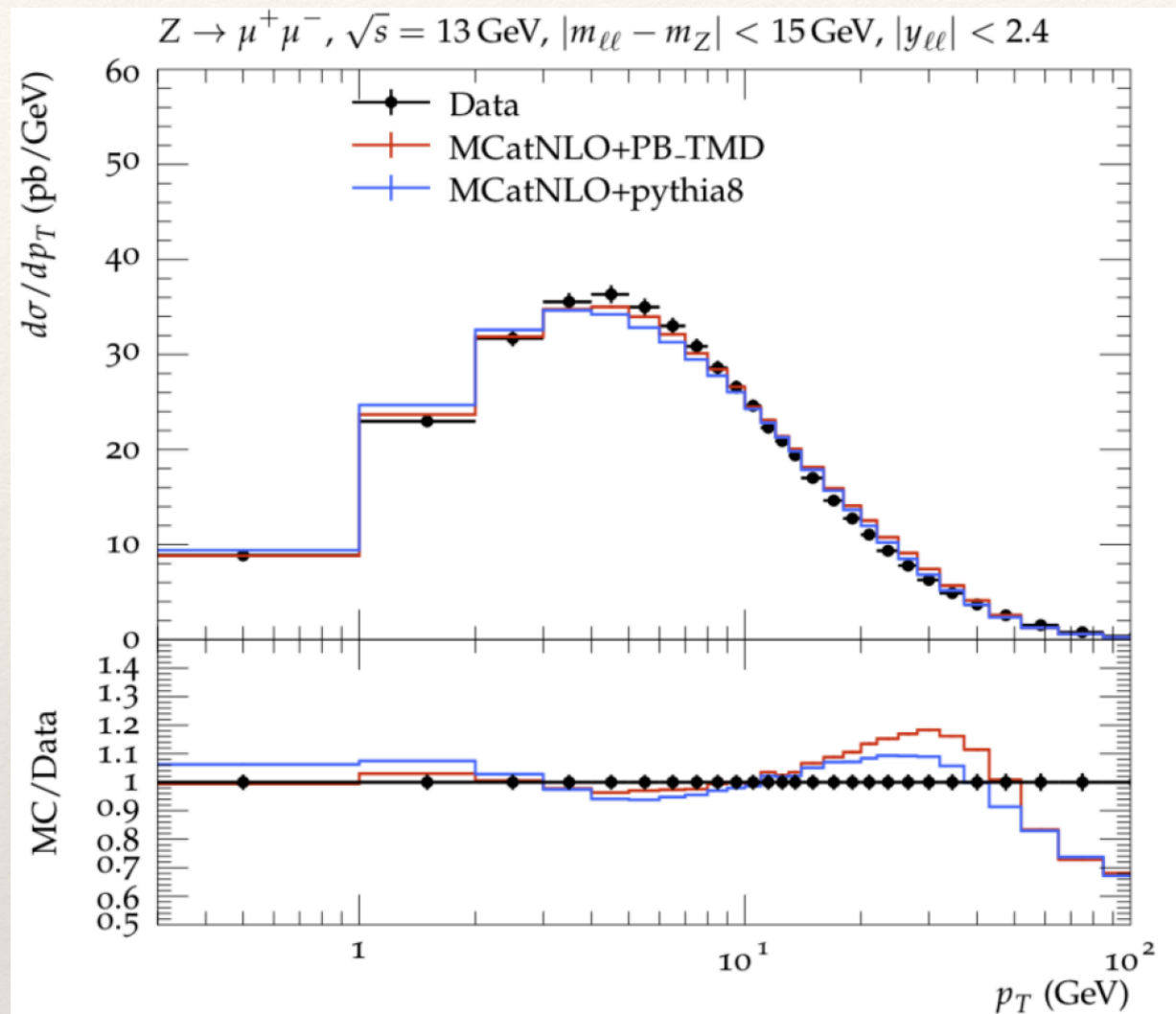
- ❖ The intrinsic kT is included in starting distribution:

$$A_{0,b}(x, k_T^2, \mu_0^2) = f_{0,b}(x, \mu_0^2) \cdot \exp(-|k_T^2|/2\sigma^2)/(2\pi\sigma^2)$$

change width $\sigma^2 = q_s^2/2$ of Gauss distribution (default $q_s = 0.5 \text{ GeV}$).

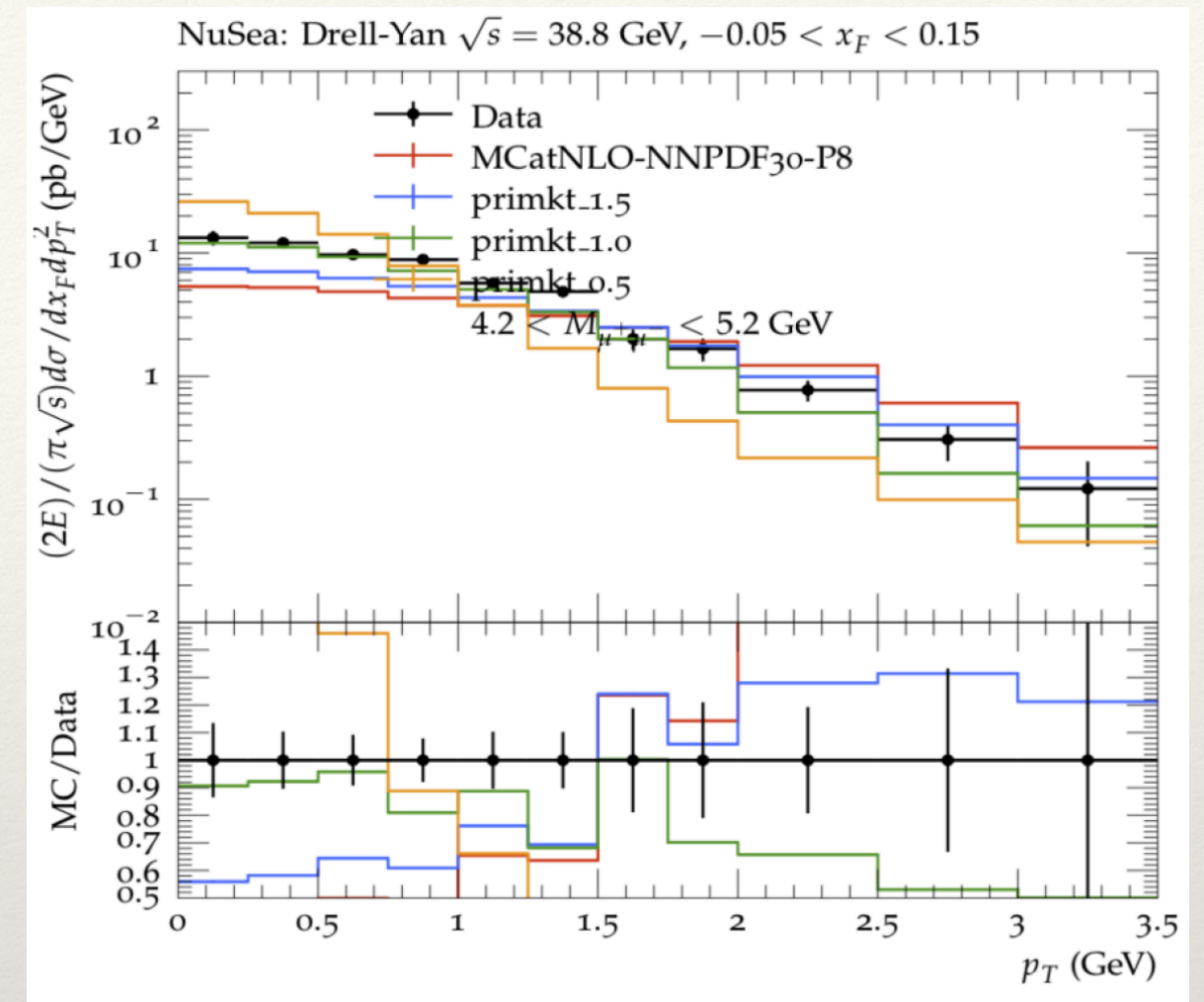
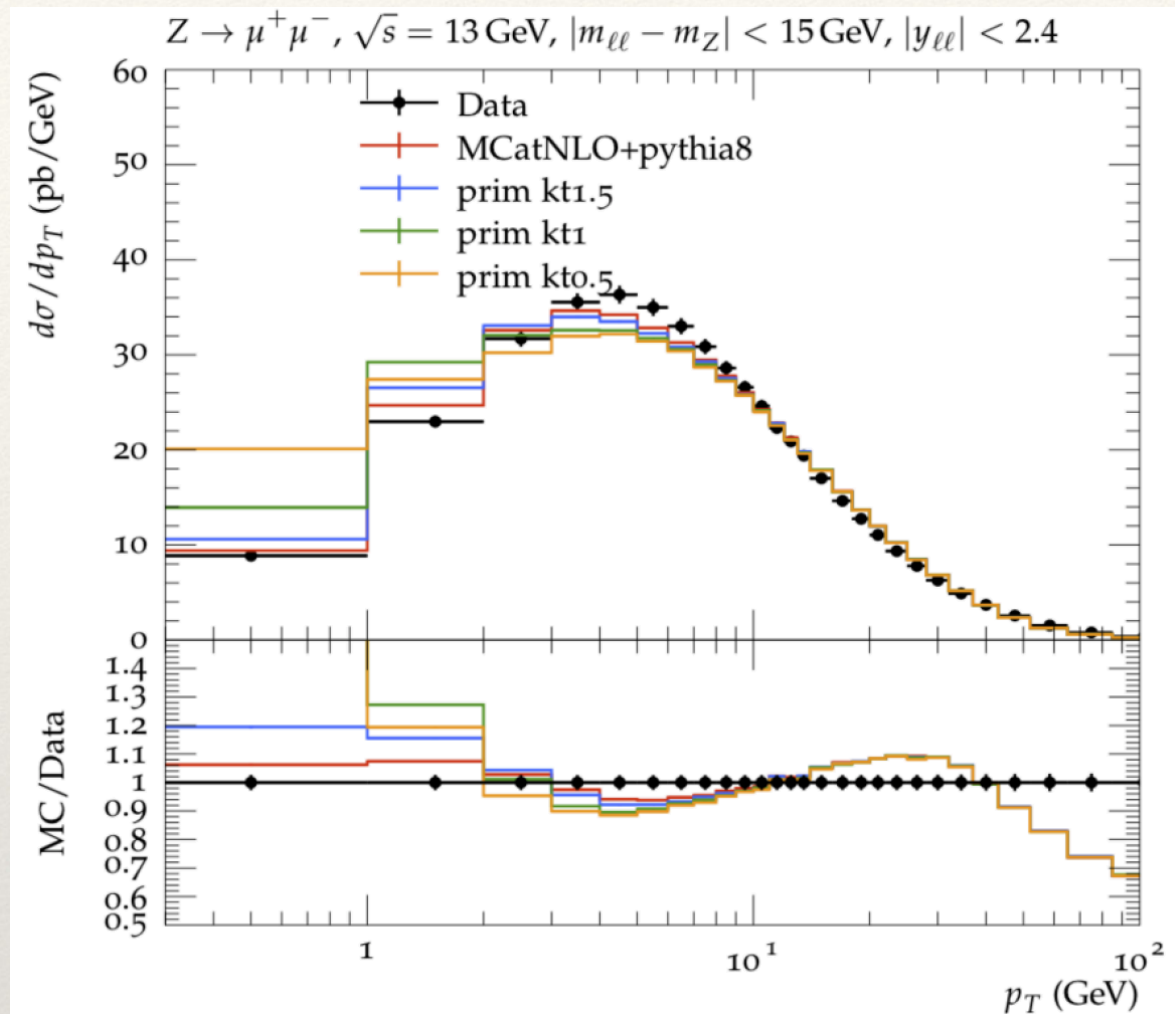


Predictions from MCatNLO+PYTHIA8



- ❖ Differences observed using Monash tune in pythia8
 - ❖ Pythia8 too high at high energy
 - ❖ Pythia8 too low at low energy

Predictions from MCatNLO+PYTHIA8



- ❖ Differences observed using Monash tune in pythia8
 - ❖ Intrinsic kT in pythia8 cannot be simply tuned to describe both high and low energy data